Departament d'Ecologia
Universitat de Barcelona

Ter River influence on Sau Reservoir limnology
Empirical and watershed-scale modeling

La influència del riu Ter en la limnologia de l'embassament de Sau
Modelització empírica i a escala de conca

Rafael Marcé Romero

TESI DOCTORAL

Departament d'Ecologia
Universitat de Barcelona
Programa de doctorat: Ecologia Fonamental i Aplicada
Bienni 2000–2002

Ter River influence on Sau Reservoir limnology
Empirical and watershed-scale modeling

Memòria presentada per Rafael Marcé Romero per optar al grau de Doctor per la Universitat de Barcelona

Rafael Marcé Romero
Barcelona, a 26 de març de 2007

Vist i plau del director de la Tesi

Dr. Joan Armengol Bachero
Catedràtic del Departament d'Ecologia
Universitat de Barcelona

Part I

RIVER INFLUENCE ON RESERVOIR LIMNOLOGY

Chapter 1

A neuro-fuzzy modeling tool to estimate fluvial nutrient loads in watersheds under time-varying human impact

1.1 Introduction

Cultural eutrophication assessment and control are amongst the most important issues natural-resource managers must face, markedly in watersheds where agricultural practices involve intensive use of fertilizers (Halweil 2002). Excess of man-induced nutrient loading into rivers has not only driven freshwater eutrophication (Vollenweider 1968; Heaney et al. 1992; Reynolds 1992), but also degradation of coastal areas and resources at a global scale (Walsh 1991; Alexander et al. 2000; McIsaac et al. 2001). Despite other factors playing a role, diversion of nutrient inputs often leads to the improvement of water quality and the lessening of negative impacts of eutrophication (Reynolds 1992). Thus, the evaluation of river nutrient loads is of great importance in supporting water management decisions in polluted watersheds.

Frequently, it is possible to estimate the fluvial nutrient load to a water body over periods of several years or decades, allowing not only the definition of realistic target situations for managers, but also a better understanding of the effects of human activities over the watershed. In most situations, such load estimates (i.e. the sum of the product of constituent concentration and flow, over a given period of time) are calculated from high frequency river flow data (i.e. daily), while river nutrient concentration data are generally scarce, weekly at best. Several methods to calculate nutrient loads have been proposed to deal with such datasets (*see* Cohn [1995] for a review). Amongst the most popular are the ratio estimators (REs) and the rating curves (RCs). REs, based on the sampling theory (Cochran 1977), assume a constant ratio between constituent concentration and flow. If certain statistical assumptions are fulfilled, they perform well in a broad range of hydrological situations, basin sizes, and flow versus nutrient concentration rela-

tionships. They can also work with low nutrient sampling resolution. For details and examples see Dolan et al. (1981), Richards and Holloway (1987), Webb et al. (1997), Preston et al. (1989), and Muckhopadhyay and Smith (2000). On the other hand, RCs build a continuous nutrient concentration trace (i.e. daily) from an empirical log-log relationship between available data on nutrient concentration and flow. Indications for their correct application and various modifications on the original method are found elsewhere (Dolan et al. 1981; Ferguson 1986, 1987; Cohn et al. 1989; Clarke 1990; Gilroy et al. 1990; Cohn et al. 1992; Cohn 1995; Lennox et al. 1997; Webb et al. 1997, 2000; Phillips et al. 1999; Robertson and Roerish 1999; Clement 2001).

When calculating loads for long periods (i.e. years or decades), the assumption of a constant nutrient concentration versus flow relationship assumed by RC and RE methods is not always realistic, due to the presence of non-linear dynamics in the relationship. This is particularly true in watersheds of developed countries, where land and water uses have experienced dramatic changes during the last decades (*see* CENR [2000] for an example). Different solutions have been proposed to calculate loads in such situations. The most simple and widely applied solution is to use the methods listed above on portions of the dataset with homogeneous nutrient concentration versus flow relationship (Preston et al. 1989; Clement 2001). This technique, however, has several drawbacks: it needs subjective decisions when grouping the years, and inference in the limits of each relationship is uncertain, usually resulting in unrealistic steps in the final load time-series. Van Dijk et al. (1996) proposed a moving-window approximation, in which regression models were successively fitted to data grouping years in a moving-average fashion. However, estimates for the final period of calculation tend to be significantly biased (Stålnacke and Grimvall 2001). Cohn et al. (1992) used multivariate regression to account for time trends and seasonality. Limitations of their approach will be outlined later in this paper. Stålnacke and Grimvall (2001) used a refinement of the application of several linear regressions, but their approach only accounts for linear relationships, and the risk of overfit is not clearly managed. Other authors (Hipel 1985; Vecchia 1985; Zetterqvist 1991) proposed using time series analysis (e.g. transfer functions and autoregressive models). Despite the robustness of some of these applications, using time series analysis on a given series is a difficult and time-consuming task, because the number of possible models is very large. Also, a high degree of expertise is needed to apply these analyses (Legendre and Legendre 1998), and available data is not always suitable for working with these approaches, mainly because the sampling time step is seldom constant. Thus, the applicability of time-series analysis methods is very restricted.

The aim of this paper is to present neuro-fuzzy modeling as an alternative tool for calculating long-term fluvial loads in watersheds where flow versus nutrient concentration relationships are strongly non-linear and uncertain due to the human impact history. The application of neural networks to modeling non-linear relationships in aquatic sciences has grown rapidly during the last three decades (Lek et al. 1996; Lek and Guégan 1999; Maier and Dandy 2000). However, one of its main disadvantages is that neural networks act as black-box inference machines. Fuzzy logic sets, on the other hand, are based on transparent, editable linguistic rules, and establish a practical framework to include human expertise into modelization (Borri et al. 1998). In this paper, we merged the fuzzy logic approach with the ability of learning algorithms from neural networks to empirically adjust a model to an input-output problem. We applied this approach, and the RC and RE methods, to calculate historical nutrient loads in two watersheds under strong human impact, to show advantages of the neuro-fuzzy approach over the other methods.

Neural networks and fuzzy logic methods are little used in limnology, and almost completely ignored in classical statistics textbooks. Moreover, standard statistical packages do not implement these procedures. To avoid these limitations, and to offer an open technique (avoiding ad hoc solutions which are difficult to implement in different scenarios), we provide a MATLAB application to calculate annual

loads using the method presented here. Recommendations are also given for its correct use.

1.2 Materials and Procedures

1.2.1 Materials

We modeled two long-term river nutrient concentration series in two watersheds with environmental problems related to human activities, i.e. eutrophication of Sau Reservoir in the watershed of Ter River (Spain), and Gulf of Mexico hypoxia in the mouth of the Mississippi River (USA).

Ter River watershed: eutrophication of Sau Reservoir

Sau Reservoir was first filled in 1963 in a middle stretch of the Ter River (Fig. 1.1A), as part of a multi-use scheme, including hydroelectric power, agricultural irrigation, domestic and industrial water supply to metropolitan areas, and recreational activities. Sau Reservoir drainage basin is a 1380 km^2 populated area (109 $people\ km^{-2}$), mainly covered by woodland (78%) and agricultural land (16%). Ter River median flow is 10 $m^3\ s^{-1}$. Since the Sau Reservoir was built, the water body experienced a process of increasing eutrophication (Vidal and Om 1993), from moderately eutrophic during the first years, to severe eutrophication in the late 1980s. Several human activities in the basin contributed to the process: intensive use of fertilizers, pig and stock farming development, proliferation of industrial areas, and changes in land use (Sabater et al. 1990; Sabater et al. 1991; Vidal and Om 1993; Sabater et al. 1995; Espadaler et al. 1997). Wastewater treatment plants (WWTP) were built in main urban and industrial areas during the early 1990s (Vidal and Om 1993), leading to a moderate improvement of the water quality of the reservoir.

Limnological characterization of Sau Reservoir started in 1963, conducted by the local water supply company (Aigües Ter-Llobregat, ATLL). Thus, a good database is available on both changes in the water body and on incoming materials through the main inflow (the Ter River, which accounts for 85% of land drained by Sau Reservoir). Total phosphorus (TP) river concentrations were used to estimate phosphorus loads to the reservoir. Analysis for TP in Ter River at Roda de Ter (Fig. 1.1A) was initiated in 1972. Sampling was weekly to monthly, and no stratification upon flow or season was applied (i.e. the sampling frequency was independent of flow or season). There are three gaps in the series: year 1983 and year 1986, and the period 1991–1994 (both inclusive). These years were not included in the final load histories. A total of 414 samples were analyzed for TP concentration (Fig. 1.2A), using the alkaline persulfate oxidation method (Grasshoff et al. 1983).

The government water agency (Agència Catalana de l'Aigua, ACA) supplied the daily averaged flows for the period 1972–1997 (Fig. 1.2A) measured at

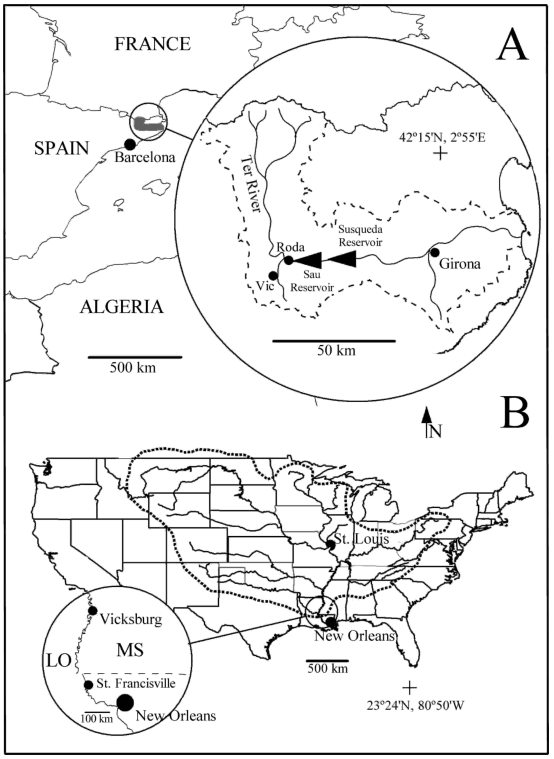

Figure 1.1 – (A) Location of the Ter River watershed and Sau Reservoir. (B) Location of the Mississippi River watershed and of sampling points.

a gage-station located 1 *km* upstream from the *TP* sampling point. From 1998, daily flows are estimated by ACA from water budgets of Sau Reservoir. No significant differences were found between gage-station estimates and water-budget estimates calculated for years prior to 1998.

Mississippi watershed: hypoxia in the Gulf of Mexico

Since the early 1980s, much attention has been paid to the hypoxia forming in front of the coast of Louisiana, and many efforts have been focused on finding causes and solutions for the observed oxygen depletion (CENR 2000). Authors have reported a direct relationship between nitrate load from the Mississippi River, which has increased over the last decades, and hypoxia development in the Gulf of Mexico (Goolsby et al. 1999; CENR 2000; Goolsby and Battaglin 2001). The Mississippi watershed is 3 208 700 km^2, with a population density of 22 $people\ km^{-2}$. Main land covers are agricultural land (58%), barren land (21%), and woodland (18%). Median flow in the Mississippi River is 14 896 $m^3\ s^{-1}$.

We estimated nitrate load in the lower Mississippi River for the period 1955–1997. River nitrate concentration data at St. Francisville (Fig. 1.1B) were obtained from the USGS National Water Information System, a public-domain computerized database (USGS Station Number for St. Francisville: 07373420). Sampling for nitrate was 6 to 15 times per year. Total number of samples was 753 (Fig. 1.2B). Nitrate was analyzed by the phenoldisulfonic acid method (Rainwater and Thatcher 1960) prior to the early 1970s, and by an automated cadmium reduction method afterward. Goolsby and Battaglin (2001) confirmed that the change in method had no systematic effect on the data, and data for the whole period were treated together. Mean daily streamflow data at Vicksburg (Mississippi) for the period 1955–1997 (Fig. 1.2B) were obtained from the USGS database (USGS Station Number for Vicksburg: 07289000).

1.2.2 Procedures

We applied three different approaches to nutrient load calculations in the two modeled basins, in order to compare advantages and limitations of classical procedures and the new method presented here. Loads were estimated with software that implements classical RC and RE methods; with a modified multivariate RC accounting for time trends; and with the proposed neuro-fuzzy inference system.

FLUX software

The FLUX software was developed by the US Army Corps of Engineers (Walker 1996), as part of a package written to bring procedures for eutrophication assessment and prediction. FLUX is available at no cost at `http://www.wes.army.mil`. The program is used to estimate nutrient loads, or other water quality components, going through a tributary sampling station over a given period of time. Using six calculation techniques (Table 2.1 *in* Walker [1996]), FLUX applies the flow versus nutrient concentration relationship developed from the sample record onto the entire flow record to calculate total mass discharge and associated error statistics, calculated by a jackknife procedure (Walker 1996). The program includes the option of stratifying the data, i.e. grouping the data upon flow and/or season. It also offers a variety of graphic and tabular output formats to assist the user in evaluating data adequacy, and in selecting the most appropriate calculation method and stratification scheme for each application. The procedure to calculate nutrient loads in the two systems under study was as follows:

1. The series was split into segments considered homogeneous regarding the nutrient concentration versus flow relationship (a bilogarithmic linear regression was applied). We calculated loads for groups of consecutive years if no significant time-trend was present in the residuals.

2. The optimal calculation method and stratification scheme was then applied to each group of

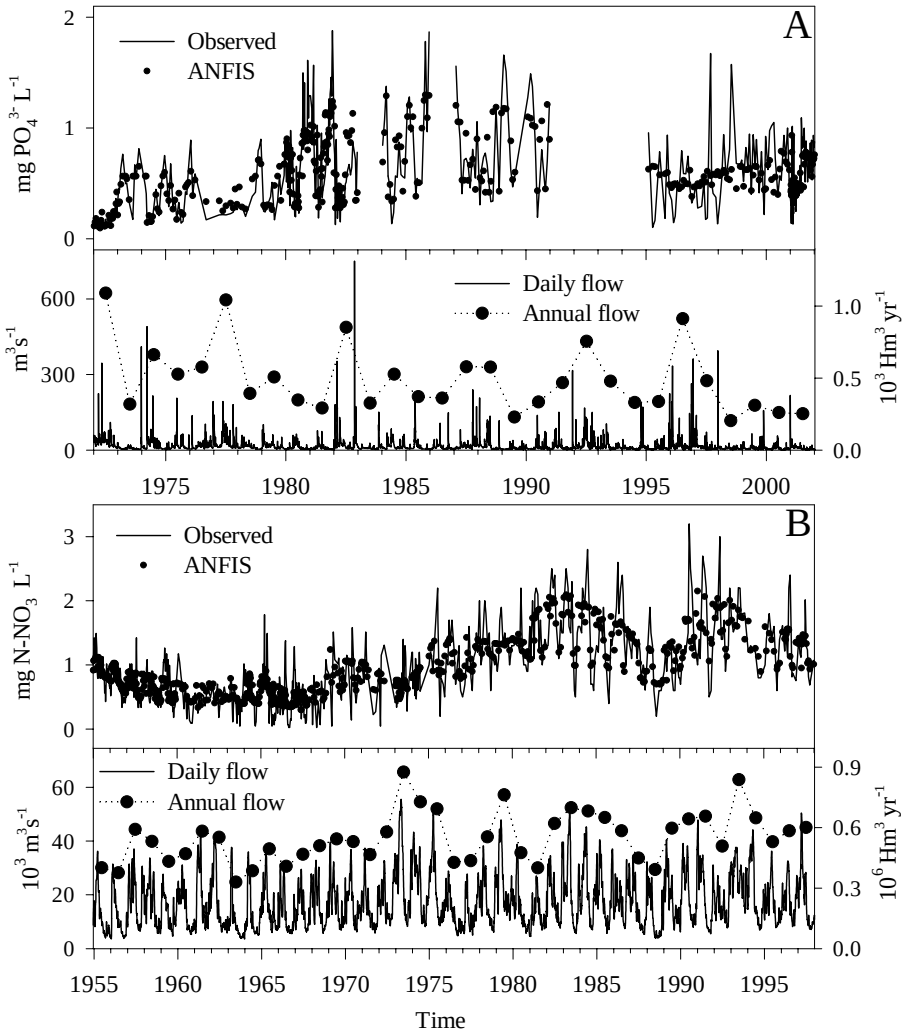

Figure 1.2 – Observed time-series of river nutrient concentration and flow in (A) the Ter River, and (B) the Mississippi River. Top figure in each panel shows the observed river nutrient concentration and the corresponding ANFIS reconstructed time-series. Each dot is the mean value for 1000 iterations. Bottom figure in each panel shows the daily mean flow (left axis) and the annual flow (right axis) for the studied period. Ticks in time axes represent the January 1.

data, considering multiple criteria, i.e. suitability of the method to data, residual analysis and standard deviation in load calculations (for details on decision making *see* Walker [1996]).

Table 1.1 shows methods and stratification schemes used in each segment defined by the FLUX procedure in the Ter and Mississippi rivers.

Multivariate rating curve

A single multivariate model may be used to calculate series with time-varying nutrient concentration versus flow relationships, instead of the classical multiple RCs and REs. Cohn et al. (1992) proposed a multivariate rating curve to account for nutrient concentration versus flow relationships, and time trends and seasonality in nutrient concentration, i.e.,

$$\begin{aligned} \ln C = &\beta_0 + \beta_1 \ln \frac{Q}{Q'} + \beta_2 \left(\ln \frac{Q}{Q'} \right)^2 \\ &+ \beta_3 (T - T') + \beta_4 (T - T')^2 \\ &+ \beta_5 \sin(2\pi T) + \beta_6 \cos(2\pi T) + \varepsilon \end{aligned} \tag{1.1}$$

where ln C is the natural logarithm of the constituent concentration C, Q is discharge, T is time (years) and ε is an error term. Q' and T' are centering variables that set the terms of the polynomials orthogonal (Cohn et al. 1992). β_i are empirically-estimated parameters. A minimum variance unbiased estimator was employed to correct for the retransformation bias (Cohn et al. 1989). Variances of annual loads were calculated as the sum of daily load variances plus the covariance terms (Likeš 1980; Gilroy et al. 1990). Calculations were implemented in a standard statistical package (SAS System) and a spreadsheet (Microsoft EXCEL).

Adaptive Neuro-Fuzzy Inference System

A fuzzy inference system (FIS) is a computing framework that combines the concepts of fuzzy logic, fuzzy decision rules, and fuzzy reasoning (Jang 1993; Jang and Sun 1995). The fuzzy logic theory was first formulated by Zadeh (1965) as a new way of characterizing non-probabilistic uncertainties. In contrast to the Boolean 1-0 logic, fuzzy logic also permits in-between values for any judged statement, i.e. it applies a continuous, multi-valued logic between 0 and 1. In terms of a function relating a variable with the probability associated to a judged statement (membership function (MF) hereafter), this is equivalent to replace a rectangular MF with a smoothed MF (*see* the *Numerical example.ppt* file in Appendix A). Figure 1.3 give examples of gaussian MFs, a common choice in fuzzy logic applications. The fuzzy decision rules are the way a FIS relates an input variable (say X) to an output variable (say Z). They take the form:

$$\text{If } x \text{ is } A, \text{ then } z \text{ is } B \tag{1.2}$$

where A and B are linguistic values (*low* or *high*, for instance) defined as MF in the input and output spaces. We can employ more than one variable in the premise side and construct rules such as:

$$\text{If } x \text{ is } A \text{ and } y \text{ is } B, \text{ then } z \text{ is } C \tag{1.3}$$

Fuzzy reasoning is an inference procedure used to derive conclusions from a set of fuzzy decision rules. The steps of fuzzy reasoning performed by a FIS are (Jang 1993):

1. Compare the input variables with the MFs on the premise part of the fuzzy rules to obtain the probability of each linguistic label (fuzzification).

2. Combine (through logic operators) the probability on the premise part to get the weight of each rule. For a comprehensive treatment of the use of logic operators in fuzzy logic see Jang and Sun (1995).

3. Generate the qualified consequent of each rule depending on their weight.

4. Aggregate the qualified consequents to produce a crisp output (defuzzification).

Table 1.1 – FLUX methods implemented during simulation of each period considered in the series of Rivers Ter and Mississippi.

Period grouped for calculation	Number of samples	Load estimation method*	Stratification scheme†	Standard deviation of load estimation‡
Ter River				
1972	23	Rating curve (5)	2 strata by flow	4.50
1973-1979	68	Rating curve (5)	2 strata by flow	4.40
1980-1984	120	Ratio estimator (2)	3 strata by flow/season	6.60
1985-1990	49	Ratio estimator (3)	3 strata by flow	5.80
1995-2001	155	Ratio estimator (2)	3 strata by flow	8.20
Mississippi River				
1955-1956	72	Ratio estimator (2)	3 strata by flow/season	3.50
1957-1960	117	Ratio estimator (2)	3 strata by flow/season	3.10
1961-1974	302	Ratio estimator (2)	3 strata by flow	3.20
1975-1977	36	Ratio estimator (2)	2 strata by flow	5.30
1978-1980	36	Ratio estimator (2)	2 strata by flow	4.70
1981-1986	70	Ratio estimator (2)	3 strata by flow/season	3.20
1987-1989	34	Rating curve (5)	2 strata by flow	5.00
1990-1993	44	Rating curve (5)	2 strata by flow	5.10
1994-1997	42	Ratio estimator (2)	3 strata by flow/season	4.00

*Numbers in brackets are method numbers in Table 2.1 *in* Walker (1996).
†The load estimation method is applied independently to each stratum. Flow strata are defined by a built-in procedure in FLUX (Walker 1996), and seasonal stratification is optimized by residual plots analysis.
‡Calculated by a jackknife procedure (Walker 1996) and expressed as percentage of estimated load.

Figure 1.3 gives a graphical example of fuzzy reasoning. In this case, the MF of the consequent of each rule is a constant instead of a fuzzy MF. These kinds of FIS are called zero-order Sugeno-type, and are very convenient for fitting procedures (Jang et al. 1995). The *Numerical Example.ppt* file in Appendix A contains a detailed example of fuzzy reasoning. Given an input-output problem, the construction of a FIS has two fundamental steps: the specification of an appropriate number and type (gaussian, triangular, and so on) of input and output MFs (structure identification), and the specification of the shape of the MFs (parameter estimation). While the structure identification is solved by human expertise or trial-and-error, numerical methods have been proposed to solve the parameter estimation step. Wang and Mendel (1992) reported a method based on the generation of fuzzy rules by examples from the modeled data set merged with human expertise. Buzás (2001) successfully applied this methodology to nutrient load estimations in tributaries to the Lake Balaton. In this paper, we used a different approach, which takes advantage of adaptive neural networks algorithms during fitting procedures. As stated by Jang (1993), an Adaptive Neuro-Fuzzy Inference System (ANFIS) is a Sugeno-type FIS where the MF parameters are fitted to a dataset through a hybrid learning algorithm.

ANFIS implementation

The core of the ANFIS calculations was implemented in a MATLAB environment. Functions from the Mathwork's MATLAB Fuzzy Logic Toolbox (FLT) were included in a MATLAB code programmed by the authors, to apply the ANFIS load estimation in a Monte-Carlo framework, and to obtain diagnostic analyses. The code to implement ANFIS, a step-by-step manual, and recommendations for potential users are in Appendix A.

For load calculations with ANFIS, the same problem was considered for the two scenarios. We defined the mean daily flow and time (expressed as number of days since January 1 of the first year in the dataset) as inputs. The output was the constituent concentration (TP for Ter River and nitrate for Mississippi River).

The structure identification was solved applying a trial-and-error procedure and a conservative cri-

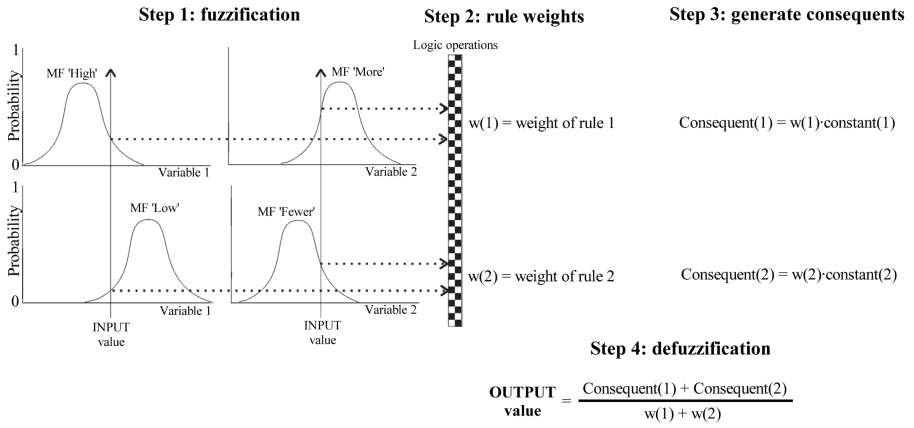

Figure 1.3 – Steps during fuzzy reasoning. The example consists in a zero-order Sugeno type FIS (*see* text for details), with two inputs, one output, and two if-and-then rules. Each input space has been characterized by two intuitively labeled gaussian MF, drawn separately for clarity and to give graphical representation of each rule. The reader should start reasoning from assigned values to inputs, and then follow arrows and explanations in the text.

terion (i.e. minimum number of parameters to the best fit). Consistent with this, gaussian MFs were used in the input spaces, as only two parameters suffice to define this curve. The ANFIS function of the MATLAB FLT was used to solve the input-output problem above with different numbers of input MFs, using all data available. An estimate of the mean square error between observed and modeled values were computed for each trial, and the best structure was determined considering a trade-off between the mean square error and the number of parameters involved in computation. Input MFs were linked by all possible combinations of if-and-then rules (Eq. 1.3), defining an output constant for each rule. Details on this procedure are given in the *User Manual.pdf* and *Numerical Example.ppt* files in Appendix A. In the Ter River case this procedure gave 6 MFs in each input (36 rules and output constants), whereas in the Mississippi River gave 15 MFs in the 'Time' input and 4 MFs in the 'Flow' input (60 rules and output constants).

Once the FIS structure was identified, the parameters that had to be estimated (gaussian input MF parameters and output constants) were fitted by the hybrid learning algorithm (HLA hereafter) implemented in the ANFIS FLT function. To avoid overfitting problems during the estimation, the data set were randomly split into two sets: a training set ($2/3$ of the data), used by the HLA to fit; and a checking set ($1/3$ of the data), which was not used by the HLA. When both checking data and training data were presented to ANFIS, the FIS was selected to have parameters associated with the minimum checking data model error.

There is no analytical expression to calculate variances of loads obtained through ANFIS. To solve this limitation, and also to avoid biases that could arise by using only one random sample, the inference procedure explained above was implemented in a Monte-Carlo sampling framework. The database was randomly resampled without replacement 1000 times, maintaining the ratio between training and checking sets. Thus, 1000 daily concentration series were generated, and consequently we obtained 1000 annual load estimates for each year. The unbiased annual load for each year was the average of the corresponding 1000 loads, and precision values were calculated as the variance of associated distributions. Ten of the 24 collections of 1000 annual load estimates in the Ter River sce-

nario showed non-normality (Kolmogorov-Smirnov test p-value < 0.05). However, the small deviation of the median respect to the average (2.4%, $n=10$) suggested that the average was an unbiased parameter of the central tendency, and indices of bimodality were present only in years 1977 and 2000. In the Mississippi River calculations, six of the 43 collections of 1000 annual load estimates showed non-normality (Kolmogorov-Smirnov test p-value < 0.05), but the small deviation of the median respect to the average (0.6%, $n=6$) also suggested the average was an unbiased parameter of the mean, and no bimodal distribution was observed.

The performance of ANFIS estimation mainly depends on the completeness of the database (Costa Branco and Dente 2001). However, when dealing with nutrient load calculations, this pre-requisite is difficult to achieve, as samples for nutrient analysis are usually comparatively scarce. In such situations, information holes in the fuzzy model could appear resulting in nonsense values in the modeled series (i.e. negative nutrient concentrations or values several orders of magnitude above the maximum concentration found in the river). These nonsense values represented an average of 1.8% of the modeled values from data of the Ter River (nonsense values from gaps included), and an average of 0.99% from data of the Mississippi River. Nonsense values were replaced by the nutrient concentration of the preceding day in the modeled series.

1.3 Assessment

The assessment of the new method for estimating fluvial nutrient loads was divided into four steps: (1) a comparison between the nutrient concentration time-series obtained with the three procedures. All methods to calculate nutrient loads directly (ANFIS, RCs) or indirectly (REs) use a predicted daily nutrient concentration time-series. Despite the fact that nutrient concentrations are not the target of these methods, this underlying calculation is of great importance, because a poor performance predicting nutrient concentrations will lead to a poor performance predicting loads. (2) A comparison between the nutrient load time-series predicted by the three methods. (3) A performance statistical analysis of the ANFIS approach, as a non-relative way to assess the ability of ANFIS calculating loads; and (4) an examination of the ability of the fuzzy modeling transparent rule feature to explain changes in the nutrient concentration versus flow relationship, because straightforward interpretation of estimated parameters is considered one of the main features of the new technique.

1.3.1 Nutrient concentration time-series comparison

Table 1.2 summarizes the results obtained comparing the observed nutrient concentration time-series (Fig. 1.2) with the time-series calculated by the three load calculation methods. The ANFIS time-series (Fig. 1.2) was the result of averaging the 1000 daily time-series obtained in each case. As shown in Table 1.2, the method that best fitted the observed data was ANFIS.

We also carried out residual trend analyses to detect systematic departures from observed time-series. The Kendall rank coefficient non-parametric test (Sokal and Rolf 1995) was used to detect trends in the residuals, because these showed significant departure from normality (Table 1.2) (Peters et al. 1997). ANFIS did not show any significant trend in the residuals. By contrast, both FLUX and Cohn methods showed significant systematic departures. It should be stressed that the application of FLUX method avoided trends in the residuals within each calculation group (Table 1.1), but this did not avoid systematic departures when looking at the whole period (Table 1.2).

Despite Cohn's multivariate rating curve was statistically significant in both cases (p-value < 0.05), the low explained variance and results from residual analyses for the Mississippi River case suggested model misspecification. The plotted time-series of nutrient concentrations sampled from the Ter River (Fig. 1.2A) described a parabolic-like curve, which could be well fitted using a quadratic polynomial such as Equation 1.1. The complex time-series sampled from the Mississippi River (Fig. 1.2B) could

Table 1.2 – Performance of the tested methods predicting daily river nutrient concentrations in the Ter and Mississippi rivers*

		Residual trend analysis			
Method	**Explained variance (r^2)**	**Residuals versus time†**	**Residuals versus flow†**	**Residuals versus predicted values†**	**Test for normality‡**
Ter River					
ANFIS§	0.60	0.18	0.38	0.49	<0.01
FLUX	0.52	<0.05	<0.001	0.31	<0.001
Cohn	0.51	0.34	0.16	0.31	<0.001
Mississipi River					
ANFIS§	0.63	0.14	0.39	0.15	<0.001
FLUX	0.58	0.21	<0.01	0.43	<0.05
Cohn	0.33	<0.001	<0.001	<0.001	<0.01

*The whole period is considered in each case.
†*P* value of the Kendall rank coefficient test for presence of trends in the residuals. H_0 = no trend.
‡*P* value of the Kolmogorov-Smirnov test for normality of the residuals. H_0 = normality.
§Average nutrient concentration for the 1000 ANFIS time-series generated (Fig. 1.2).

not be modeled by a quadratic fit, leading to spurious predictions. Despite results of the diagnosis analysis, we applied the model over the entire series (i.e. without splitting it), in order to illustrate the effect on final results of the highly non-linear nutrient concentration versus flow relationship in this system. Thus, poor performance of the method reported in this case should not be considered as negative criticism of the method itself, but as limiting its applicability.

1.3.2 Nutrient load time-series comparison

Figure 1.4 shows the nutrient load time-series in Ter and Mississippi rivers, calculated by the three methods under comparison, expressed as flow-normalized annual nutrient load and standard deviation. To compute flow-normalized loads:

$$Flow\ norm.\ load_i = \frac{Actual\ load_i}{Q_i} Q' \qquad (1.4)$$

where $Actual\ load_i$ is the predicted load in year i, Q_i is the annual flow in year i, and Q' is the mean annual flow for the whole period. Flow-normalization eliminates the effect of the varying hydrology in the time-series plot. This makes the figure more readable, it allows the interpretation of the changes in the flow-normalized loads as indications of changes in the man-induced loading, and better reflects the underlying nutrient concentration versus flow relationship (Stålnacke et al. 1999; Stålnacke and Grimvall 2001).

As shown in Figure 1.4, results regarding general patterns of the series differ in the two rivers. While in the Ter River the three methods gave similar results, (i.e. increasing nutrient load from 1972 to 1990, and decreases afterwards), the Cohn's approximation gave dramatically different results to the other two methods on the Mississippi River calculations. This result is a direct consequence of the poor performance of Cohn's method predicting nutrient concentrations in the Mississippi River (Table 1.2). Cohn's model may be applied in such situation splitting the series into fragments that can be quadratically fitted (*see* Goolsby and Battaglin [2001]), procedure equivalent to that applied in the FLUX software. Increasing the degree of the polynomial in Cohn's equation did not give acceptable results (*see* Figure 1.4B and Appendix B for derivation). Moreover, processing time and mathematical derivations increase formidably with the degree of the polynomial. Therefore, although Cohn's ap-

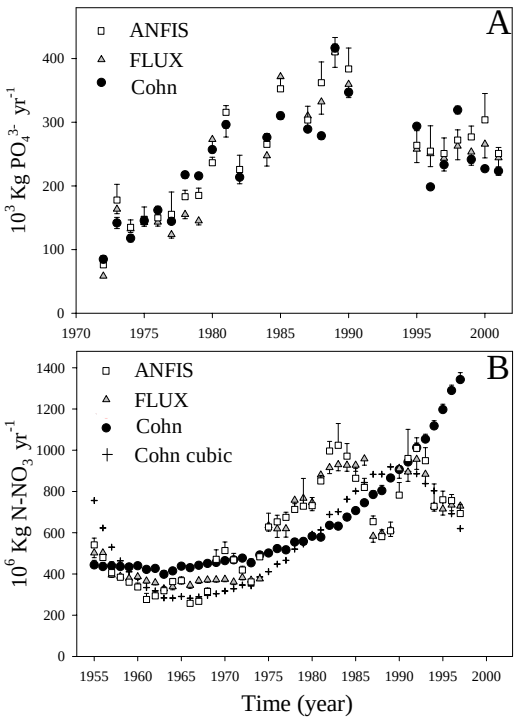

Figure 1.4 – Flow-normalized annual nutrient loads and standard deviation calculated through ANFIS, FLUX, and Cohn's procedures. (A) Results for the Ter River and (B) for the Mississippi River. Results applying a cubic modification of Cohn's approximation are also shown in panel (B). For clarity, only one error bar is represented for each symbol. Many error bars are unappreciable.

proximation could work in some cases, its applicability is limited.

ANFIS and FLUX calculations were both good in both scenarios. Detailed analysis, however, revealed the well-known step artifact in the FLUX series. Each transition between years modeled in different calculation groups (*see* Table 1.1) corresponds with a step in the final series. The artifact occurs in both plots, but is more evident in the Mississippi River FLUX series (*see*, for example, transition between years 1974–1975, 1977–1978, or 1986–1987). A step in the series could correspond with a real change in the river (in fact, some of the steps are followed by the ANFIS calculation), but the absolute correspondence between steps and transitions give strong evidence of presence of artifacts. By contrast, ANFIS applies a single method through the entire series avoiding the presence of artifacts (i.e. steps) in the final load histories. This adaptability to different situations and empirical relationships is possible due to two important features of the ANFIS approximation: (1) it is a model-free methodology and, (2) it acts as a local inference machine.

On the other hand, the FLUX and Cohn's approximation give averaged dispersion values, as the models are fitted to a group of years, or the entire series. Thus, interpretation of the standard deviation of individual annual loads is not straightforward. In contrast, the ANFIS method gives dispersion values independently calculated for each year. Thus, we can interpret standard deviations as annual uncertainties. It should be stressed that differences in annual uncertainty could arise from both the varying relationship between flow and nutrient concentration, and uncertainty caused by the different number of samples available for each year. Although no consistent relationship was found between number of samples and ANFIS calculated uncertainty in this study, this could not be the case in other situations. Thus, interpretation of ANFIS dispersion values as uncertainty in the flow versus nutrient concentration relationship should always take in consideration the effect of the sampling frequency. In any case, the possibility of analyzing these features of the data with annual independent calculated values is a great advantage of ANFIS over other procedures.

1.3.3 Performance of the ANFIS estimation

The validity of load estimations based on FLUX methods and the multivariate rating curve by Cohn et al. (1992) have been tested and confirmed on numerous occasions (Dolan et al. 1981; Richards and Holloway 1987; Preston et al. 1989; Clarke 1990; Cohn et al. 1992; Webb et al. 1997; Phillips et al. 1999; Muckhopadhyay and Smith 2000). To test the performance of ANFIS in calculating loads, we ap-

plied a split-sampling approach similar to that used by Preston et al. (1989) and Cohn et al. (1992).

The ANFIS method was tested separately at both sampling sites. The complete records of daily flow, time and nutrient concentrations were randomly subsampled under different frequencies to obtain training and checking sets of different sizes (training set was $2/3$ the sampled set; checking set $1/3$ the sampled set). Data not included in the preceding sets constituted the evaluation set. The two first sets were used to train the ANFIS, using the model structures presented in subsection *Procedures*. Then, input data in the evaluation set was used to model a sum of loads with the FIS that were compared to the true sum of loads contained in the output of the evaluation set. Subsamples of the training + checking sets were of 50 samples, and calculations were repeated with 50 more samples in these two sets until the maximum number of samples in the original data set was reached. One hundred different calculations were done for each frequency. Nonsense values, as a result of inference from non-trained inputs, were eliminated and not replaced. They were registered and not used in final calculations.

The mean percentage bias between the sum of loads estimated and the true sum of loads was calculated as follows:

$$B_x = \left(\sum_{i=1}^{100} \left[100 \times \left(\frac{L_{e,i} - L_{r,i}}{L_{r,i}} \right) \right] \right) / 100 \qquad (1.5)$$

where B_x is the mean percentage bias for a given sampling frequency x, $L_{e,i}$ the estimated sum of loads for the ith random sampling, and $L_{r,i}$ the true sum of loads for the ith random sampling. The statistical significance of the difference between the estimated sum of loads and the true sum of loads was tested with the Mann-Whitney U test (Sokal and Rolf 1995).

Table 1.3 shows the results obtained from the performance analysis of ANFIS estimation. In the Ter River scenario the mean percentage bias gave non-significant values with 300 samples in the training + checking sets. Thus, we considered load calculations in the Ter River as unbiased (Fig. 1.4A, 414 samples). With fewer samples, calculations were significantly biased, markedly with fewer than 100 samples. The mean percentage of nonsense values during performance analysis for 500 samples (Table 1.3) coincided with the mean percentage of nonsense values reported during simulations (i.e. 1.8%).

In the Mississippi River, the ANFIS procedure worked well even with few samples in the training + checking sets, and the mean percentage bias showed non-significant values with 50 samples. Consequently, load calculations in the Mississippi River (Figure 1.4B, 753 samples) were also considered as unbiased. The mean percentage of nonsense values during performance analysis for 700 samples was slightly higher than the percentage found during simulations (i.e. 0.99%). This is likely due to the effect of the reduced number of samples in the evaluation sets (Table 1.3) compared to the number of simulated days in the load calculations (i.e. 15 706 days).

1.3.4 Ecological interpretation of ANFIS parameters

A desirable property of any model applied to real data is that the parametric structure of the model resulting from fitting procedures has physical meaning, i.e. that the model does not work as a blind fitting machine. A remarkable feature of the ANFIS approximation is that we can interpret fitted parameters. Figure 1.5 shows the effect of all input combinations (flow and time) on the outputs (nitrate and total phosphorus concentration) in Mississippi and Ter Rivers. Panels in Figure 1.5 could be interpreted as the plot of all defined if-and-then rules (*see* Eq. 1.3) in each system, but also as a plot of the evolution over time of the nutrient concentration in each flow category. Some rules were not included in the graph, because standard deviation of the associated output parameters were very high, and made the figure unreadable. This is a consequence of information holes that arise from incomplete databases. Values for output parameters should be interpreted in a relative mode, because final concentrations are generated after defuzzification procedures.

Table 1.3 – Performance of ANFIS estimation in Ter and Mississippi River scenarios (*see* text for details)*

Samples in training + checking sets	Mean percentage bias (SD)	Samples in evaluation set	Mean percentage of nonsense values (SD)
Ter River			
50	23.46*** (16.87)	364	25.8 (11.30)
100	10.90*** (13.30)	314	7.90 (4.45)
150	11.20*** (9.76)	264	4.90 (2.60)
200	6.00*** (10.10)	214	3.40 (2.47)
250	4.80** (9.65)	164	2.50 (1.77)
300	3.08ns (10.20)	114	1.90 (1.50)
350	4.42ns (11.50)	64	2.06 (1.53)
400	3.09ns (28.00)	14	1.57 (3.00)
Mississippi River			
50	–7.96ns (29.1)	703	31.63 (1.68)
100	–1.22ns (22.2)	653	26.29 (1.79)
150	–0.53ns (16.35)	603	15.42 (1.44)
200	–1.29ns (13.10)	553	8.89 (1.32)
250	–1.11ns (9.28)	503	5.72 (1.02)
300	–0.67ns (7.00)	453	4.04 (0.92)
350	–1.15ns (6.99)	403	3.37 (0.94)
400	–1.31ns (6.57)	353	2.67 (0.95)
450	–1.50ns (7.99)	303	2.25 (0.92)
500	–0.88ns (8.07)	253	1.81 (0.82)
550	–1.01ns (7.96)	203	1.56 (0.77)
600	–1.81ns (10.95)	153	1.48 (0.96)
650	–1.96ns (13.46)	103	1.41 (1.19)
700	–4.15ns (20.89)	53	1.26 (1.65)

*Statistical difference between estimated and true load: ns = not significant; ** = significant at the 1% level; *** = significant at the 0.1% level.

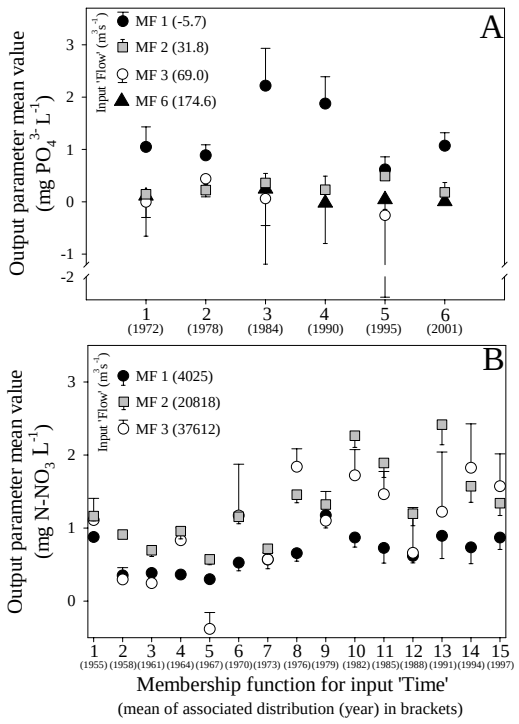

Figure 1.5 – Graphical representation of the if-and-then fuzzy rule structure obtained during nutrient load calculations in (A) the Ter River, and (B) the Mississippi River. Symbols represent the mean value assigned by the HLA for each output constant parameter using 1000 iterations, and bars are standard deviations. (For clarity, symbols corresponding to rules with very high output parameter standard error were not drawn. Also, only one error bar is represented for each symbol. Many error bars are unappreciable). The average value of the mean parameter of each gaussian MF is given in brackets. Graphics must be read as follows: if MF for Flow is [symbol] and MF for Time is [x-value] then output constant is [y-value].

As shown in Figure 1.5A, nutrient concentrations in the Ter River were higher at low flows, suggesting a dilution dynamics governed by point sources located near the sampling point. In fact, man-induced nutrient loading in the Ter River watershed is concentrated around the industrial and farming area of Vic (Vidal and Om 1993), and the main stream draining this area (Gurri River) discharges few kilometers upstream the sampling point (Fig. 1.1A). Differences between periods were more evident in the lowest flow region, with the highest phosphorus concentrations during the periods just before 1993, when WWTP were placed in the basin. Dilution dynamics was also clearer before 1993. Thus, we can hypothesize that it was a change in the relative importance of point sources as a consequence of the WWTP implementation. This hypothesis is also supported by results from observed flow versus observed nutrient concentration log-log relationships. Regression for the 1980–1990 period ($n=169$, p-value < 0.001, $r^2=0.48$) gave an intercept of 0.28 $mg\,PO_4\,L^{-1}$ and a slope of -0.47. Regression for the period 1995–2001 ($n=155$, p-value < 0.001, $r^2=0.10$) gave an intercept of 0.19 $mg\,PO_4\,L^{-1}$ and slope -0.22. Differences between both intercepts and slopes were significant (p-value < 0.001, Tsutakawa and Hewett [1978]). Considering the value of the intercept as an indication of the point sources level and the slope as an indication of the importance of the dilution effect (Behrendt 1993; Stålnacke and Grimvall 2001), this analysis supports conclusions extracted from ANFIS parameters.

Error bars and missing rules inform about the uncertainty of the ANFIS inference. Uncertainty is present in the high flow regions, poor represented in the nutrient concentration sampling. This is a consequence of the hydrology of the Ter River (Fig 1.2A), with stable low flow conditions and sudden floods typical from Mediterranean rivers. Uncertainty observed in the lowest flow region, good represented in the nutrient concentration sampling, was caused by the timing of point-sources spills, which could not be explained by flow. When WWTP were implemented in the basin the uncertainty was less pronounced, because most point sources were replaced

by a single and more constant spill.

In the case of the Mississippi River (Figure 1.5B), the uncertainty of the inference system also accumulated in the high flow regions. This is clearly shown by the standard deviation of the output parameter mean values and missing rules. This suggests that more sampling effort is needed during high flow periods. Nutrient concentration values were systematically higher at intermediate flows, suggesting non-point sources prevalence (Behrendt 1993; Stålnacke and Grimvall 2001). This is also suggested by the observed flow versus observed nutrient concentration log-log relationship ($n=714$, p-value < 0.001, $r^2=0.12$), which gave a positive slope of 0.29. In fact, runoff from agricultural land is thought to be the main nitrogen input to the Mississippi River (CENR 2000). Output parameter mean values followed an increasing trend (specially at intermediate flows), which is in agreement with the direct relationship established between the increasing amount of agricultural fertilizers applied in the basin and the nitrogen load transported by the river (Alexander et al. 2000; Goolsby and Battaglin 2001; McIsaac et al. 2001).

1.4 Discussion

Solutions available to calculate long-term loads in watersheds under time-varying human impact have several limitations. The most important are solved by the new method proposed here. The following is a list of the main advantages of the new technique:

1. ANFIS is a model-free, easy to implement approach. In contrast to time-series methods, little training is needed to calculate loads with ANFIS (*see* Appendix A for MATLAB codes and use). ANFIS implements a single fitting procedure to complex (i.e. non-linear) situations, without the need of establishing a formal model for the problem being resolved. Thus, no a priori information is needed about the empirical relationship between the explanatory and predicted variables, and the method suitability is always tested a posteriori.

2. With customary methods, variables frequently need transforming to enclose the problem into a linear relationship. Retransformation of results into real space is not straightforward, and is dependent on the statistical properties of the constituent versus flow relationship. These properties do not always allow correct retransformation of variables, leading to significant biases (Cohn 1995). Time-series methods require a constant time step during sampling. Our method avoids these drawbacks.

3. ANFIS fits nutrient concentration time-series better than customary methods, with no systematic departure from observed data. This and the application of a single fitting procedure over the entire series avoid the presence artifacts (i.e. steps) in the final load series.

4. On the other hand, calculated dispersions with ANFIS can be interpreted as annual uncertainties. Load calculations are often the first step in eutrophication studies. The values generated during load calculations are then used to calibrate models, compare loads, and define target situations. If management decisions directly or indirectly depend on load calculations, then knowledge about uncertainty in load estimations becomes a priority (Reckhow and Chapra 1983; 1999). Using annual dispersion values calculated from a classical, empirical relationship grouping several years could be inaccurate, unless variance is constant all over the relationship and we have equal number of samples for all years.

5. Also, the ANFIS method allows interpreting the values of the parameters fitted. The transparent rule structure of ANFIS allows the user to extract information about the empirical relationship between flow and concentration over time, drawing concise explanations. This a posteriori interpretation seems preferable to the a priori constriction of the data to an empirical relationship with an often dubious physical meaning. This open-box feature makes ANFIS an attractive exploratory data analysis tool,

especially in situations were available models fail explaining observed phenomena.

1.5 Comments and Recommendations

The ANFIS procedure presented here, despite being model-free, must be implemented with care. A critical number of samples are needed in order to have significant results, and to avoid having too many nonsense values during simulation. The database must be as complete as possible, including nutrient concentration samples over a broad range of flows and times (in a classical framework, working with no-trained data would be equivalent to extrapolation). It is best to exclude large gaps in the database from final results. We do not recommend any minimum number of samples per year, because this will strongly depend on the dynamics of the system. Alternatively, we strongly recommend using the performance analysis procedure explained in the text (*see* also Appendix A), and the fit between observed and modeled nutrient concentration time-series as a definitive criterion to judge the suitability of the method. If percent bias given by performance analysis is higher than 5%, results should be regarded with caution, and biases higher than 10% should not be accepted. However, since ANFIS uses a learning algorithm, we must always work with a number of model parameters not exceeding $1/4$ the number of samples in the training sets, in order to avoid the risk of overfitting and loose of generality. This place in practice the minimum number of samples around 150.

The performance of ANFIS calculating loads strongly depends on the relationship between flow and river nutrient concentration. It should be stressed that in some rivers nutrient dynamics is independent of flow (Whitfield 1982), and that presence of large lakes and impoundments significantly alter flow and nutrient dynamics (Kelly 2001). Also, we tested our method in two basins covering a wide range of sizes, but not in very small basins where nutrient dynamics could be more unpredictable (Bernal et al. 2002). In these situations, ANFIS performance using flow as a key input variable could be low. This poses the question on how strong the relationship between flow and nutrient concentration should be. Our experience is that using regression to explore this relationship in long-term data is not optimal, because the time-varying effects mask the relationship, and usually leads to a confusing and noisy scatter graph. Our recommendation is using the no time-consuming ANFIS method as an exploratory data analysis tool, and to judge the suitability of the method on the basis of the performance analysis on nutrient load calculations. If bias in load calculations is unacceptable, the analysis of the parameters fitted and the modeled nutrient concentration time-series could give valuable information to apply alternative procedures.

As a concluding remark, we used ANFIS to solve nutrient load calculations, but this technique should also work with few modifications in a broad range of regression problems. We encourage researchers to apply and modify our codes to implement ANFIS in other situations. Also, the exploratory data analysis ability of this technique deserves more detailed studies (*see* Appendix C).

Chapter 2

The role of river inputs on the hypolimnetic chemistry of a productive reservoir: implications for management of anoxia and total phosphorus internal loading

2.1 Introduction

Most deep natural lakes from the temperate and subtropical regions develop a well-defined layered structure during summer (Wetzel 2001). The strengthening of a stable seasonal thermocline usually leads to a summer hypolimnion virtually isolated from the atmosphere. Since the runoff penetration into stratified waters tends to be small and dispersive for several reasons (runoff via low-order tributaries or diffusive sources, and interception by wetlands or littoral interface regions; Wetzel [1990]), the surface water input is not a recurrent driver on these systems during summer months (Margalef 1983). Thus, for most natural, non-manipulated lakes the biogeochemistry of hypolimnetic water during summer stratification is isolated from direct atmospheric or tributaries interactions. Lakes with significant groundwater recharge (e.g. Casamitjana et al. 1993), lakes of damming-like origin (e.g. Gibbs 1992), and large lakes with high order tributaries draining vast watersheds (e.g. Vandelannoote et al. 1999) are main exceptions.

By contrast, mainstream deep reservoirs show a relatively high drainage basin area: water body area (BA–WA) ratio (Straškraba 1998), implying a strong advective flux from the drained catchment even during the low-flow summer conditions. In these systems the horizontal component of water fluxes have a major impact on its physical, chemical, and biological dynamics (Ford 1990), to an extent that they are often considered as hybrid systems between lakes and rivers (Margalef 1983). Additionally, if the continuous river input is overloaded with nutrients and organic matter, not only hydrol-

ogy, but also the chemical load helps to define a marked longitudinal heterogeneity in the reservoir limnological characteristics (Kimmel et al. 1990). Canyon-shaped reservoirs are prototypical at this respect, because their morphology forces a very clear advective flux (Armengol et al. 1999).

Apart from these considerations, partially based in a plug-flow view of advective movements in reservoirs, one of the most striking limnological features of reservoirs (and specially in canyon-type ones) is the recurrent presence of the river water as density currents reaching the end-wall of the system (Ford 1990). This exerts a paramount effect on the vertical physical structure of the reservoir: directly affects the density gradients and magnifies the differences in residence time between different layers if the river input goes to a well delimited water parcel (Rueda et al. 2006). Nevertheless, suspended and dissolved materials coming from the watershed will also be transported in these flows, enhancing chemical and biological vertical heterogeneity. These have an important implication for hypolimnetic water biogeochemistry during stratification: if the river water enters with little entrainment directly to the hypolimnion via a density current, the dynamics of this layer will be directly forced by a driver which is essentially independent of in-lake processes. This is quite a different situation compared to classical load-response models assumptions, which implicitly suppose a lagged, indirect effect of the external forcing on the hypolimnion biogeochemistry through epilimnetic processes (Chapra and Canale 1991; Chapra 1997). All in all, not only the sediment boundary and the fluxes through the thermocline need to be considered in these advective-dominated systems. Also the tributary inflow will play a role shaping the hypolimnetic biogeochemistry (Fig. 2.1).

In this study we illustrate how allochthonous organic matter (taking the dissolved organic carbon (*DOC*) as an appropriate surrogate) and nutrients in the river inflow can exert a significant effect on the oxygen content and total phosphorous dynamics in the hypolimnion of a reservoir showing recurrent summer density currents. In such a scenario, the effect of external inputs of *DOC* and nutrients

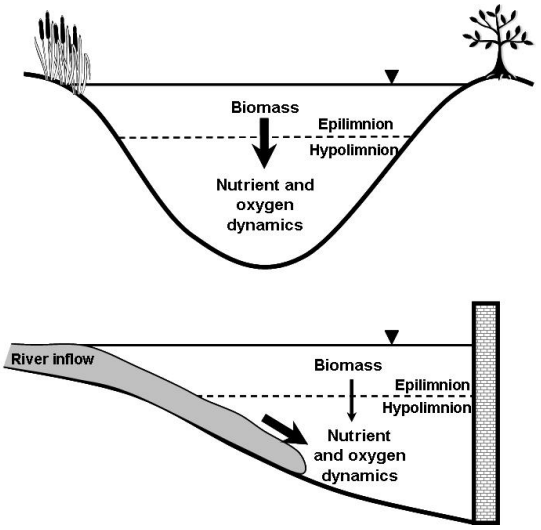

Figure 2.1 – Schematic diagram showing the relative importance of vertical and horizontal processes on hypolimnetic nutrient cycling and oxygen content in (A) natural lakes and (B) canyon-shaped reservoirs. Sediment interactions are considered as a lagged epilimnetic effect on this schema.

on the hypolimnetic biogeochemistry should be enhanced by the fact that density currents can directly inject allochthonous substances into the deep layers. Thus, the external input does not enter in the epilimnetic microbial loop, which could mask its role in the subsequent hypolimnetic oxygen depletion caused by sedimentation of epilimnetic organic matter. We empirically tested this hypothesis using long-term data from a canyon-shaped reservoir that underwent dramatic changes in the nutrient and *DOC* loading during an 11-years period, followed by an increase in the hypolimnetic oxygen content, but in which no significant trends in epilimnetic phytoplankton biomass arose. First, we illustrate the historical trend of the nutrient and *DOC* load to the reservoir, and the evolution of the hypolimnetic oxygen content. Then, an empirical regression approach is used to stress the effect of the river inputs on the biogeochemistry of the deep layers of the reservoir during summer, when anoxic conditions develop.

2.2 Materials and Methods

2.2.1 Study site

Sau Reservoir (Fig. 2.2) was first filled in 1964 in a middle stretch of the Ter River (NE Spain, 10 m^3 s^{-1} of median flow), which accounts for ca 90% of land drained by Sau Reservoir. The Ter River basin at Sau is 1380 km^2, and consists in a populated area (109 $people\ km^{-2}$), mainly covered by woodland (78%) and agricultural land (16%). Since the Sau dam was built, the waterbody experienced a process of increasing eutrophication (Vidal and Ohm 1993), from moderately eutrophic during the first years, to severe eutrophication in the early 1990s. Several human activities in the basin contributed to the process: pig farming development, intensive use of agricultural fertilizers, proliferation of industrial clusters, and changes in land use, mainly from forest and riparian strips to agricultural land (Sabater et al. 1990). Physicochemical wastewater treatment plants (WWTP) were built in the main urban and industrial areas during the early 1990s, leading to a moderate improvement of the water quality of the reservoir. During the fall 1999 the most sizeable from these WWTP (located just few kilometres upstream the reservoir) was improved with additional biological treatment. Extended limnological descriptions and detailed processes in the reservoir can be found elsewhere (Armengol et al. 1986; Comerma et al. 2001; Šimek et al. 2001; Gasol et al. 2002; Rueda 2006; Marcé et al. 2006).

Sau Reservoir is a canyon-shaped water body (Table 2.1) where river density currents are commonly observed, especially during the growing season (May to September). Although some aspects of the river circulation are difficult to simplify (e.g. location and mixing at the plunge point and entrainment with reservoir water across the reservoir; Ford [1990]), the depth of intrusion of river water in the reservoir can be reasonably well predicted from measured temperatures in the river and the reservoir, specially in systems like Sau Reservoir where water density is almost exclusively characterized by temperature (Rueda et al. 2006).

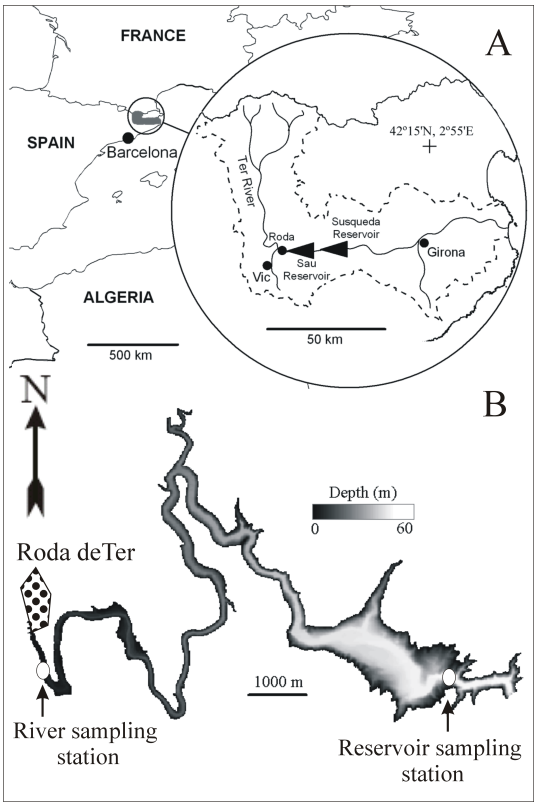

Figure 2.2 – Location (A) and bathymetric map (B) of Sau Reservoir. The river and reservoir sampling stations are depicted on the bathymetry.

Twelve years (1994–2005) of Ter River temperature observations and the corresponding temperature profiles in the limnetic part of Sau Reservoir has lead to a clear definition of the circulation pattern of the river water in the reservoir. Based on smoothed function of monthly average for the whole period, there are underflows during the first part of winter because the river water is much colder than the reservoir water (Fig. 2.3). In early spring, this situation is reversed and the river flows into the reservoirs as an overflow for a short period. In late spring, when the snow melts in the mountains, the river water temperature rises significantly slower than the reservoir surface water, and the river arrives at the end-wall of the reservoir as an interflow. This

Table 2.1 – Sau Reservoir main morphometric and hydrological data.

Variable	Value
Max. volume ($x10^6$ m^3)	168.5
Max. area ($x10^6$ m^2)	5.8
Max. depth (m)	65.0
Mean depth (m)	25.2
Max. length ($x10^3$ m)	18.0
Max. width ($x10^3$ m)	1.3
Mean inflow ($x10^6$ m^3 yr^{-1})	540.5
Mean residence time (yr)	0.3

situation will persist until the winter, when an underflow develops and the pattern is resumed. For detailed longitudinal transects and modelling results that supports the previous description see Armengol et al. (1999) and Rueda et al. (2006).

Comparing this pattern with the depth of the seasonal thermocline that develops in the reservoir (Fig. 2.3), it is apparent that during the summer months (from June to September) the river inflow always plunges deeper than the seasonal thermocline. Thus, the river inputs go directly to the hypolimnion during summer. This assertion assumes that the entrainment of river water into the surface waters during plunge and transport to the end-wall side of the reservoir is negligible in terms of the river load. Although in some situations this would not hold, for most density currents this is not an unreasonable assumption (Ford 1990).

2.2.2 Methods

The database used in this study consists on monthly samplings from 1995 to 2005, covering the main inlet (Ter River at Roda de Ter gauge station, just upstream the reservoir) and a sampling station located at the lacustrine section of the reservoir. For this station, 1 *m* vertical profiles of temperature, pH, conductivity, and oxygen concentration were measured with a multiparametric probe (Turo T-611 Water Quality Analyzer). Based on these profiles, a variable number of water samples were collected with a 5 *L* hydrographic bottle (UWITEC), in order to accurately describe the vertical heterogeneity in the sampling point. The samples were stored in dark bottles and immediately processed in a nearby laboratory where they were analysed for total phosphorus (*TP*), total nitrogen (*TN*), nitrate, ammonia, soluble reactive phosphorous (*SRP*), dissolved organic carbon (*DOC*), and chlorophyll-a (*Chl-a*). The analytical methods applied are described in Table 2.2. The sampling at the river location was identical, but consisting only on one integrated water sample. The government water agency (Agència Catalana de l'Aigua, ACA) supplied the daily hydrological and hydromorphological data of Sau Reservoir.

Constituent loads to the reservoir from the Ter River were calculated using the methodology described in Marcé et al. (2004)[1]. The calculation is based on a fuzzy logic characterization of the time-varying relationship between river flow and constituent concentration, and was specially designed to deal with rivers that undergo a variable human impact over time. The method not only gives an unbiased estimator of the load over a given period of time, but also the uncertainty expressed as a Monte-Carlo derived population of values from which distributional parameters can be calculated. Since the validity of this approach was already tested for the Ter River in Marcé et al. (2004), we refer to this paper for the detailed calculations.

The depth of the seasonal thermocline was estimated with the location of a density gradient of at least 0.15 $kg\ m^{-4}$, threshold that consistently avoided the daily thermocline or other transient structures. Water density was calculated assuming negligible effect of salinity (Krambeck et al. 1992). Epilimnetic and hypolimnetic summer constituent concentrations were calculated computing volume-weighted means for water samples and probe data collected above and below the calculated depth of the seasonal thermocline, respectively. The surface area of anoxic sediment (SAS) was computed following Nürnberg (1995) as the surface of reservoir bottom that is in contact with water containing less than 1 $mg\ O_2\ L^{-1}$).

[1] Chapter 1 in this Thesis

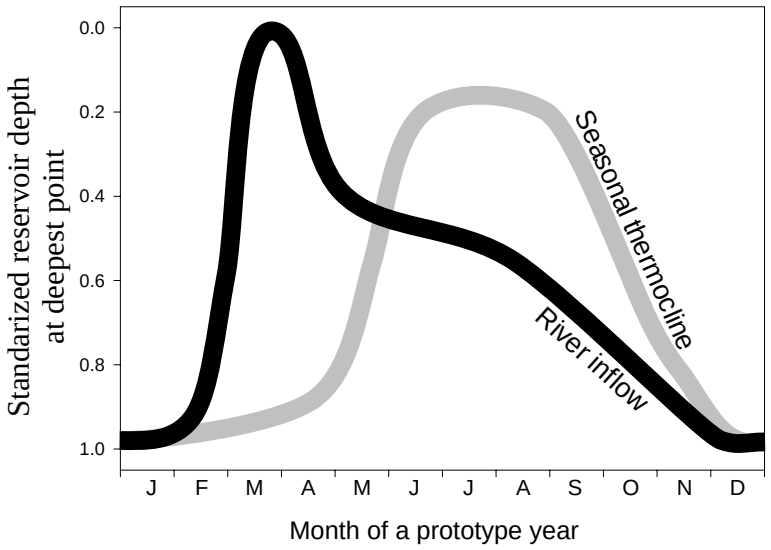

Figure 2.3 – Schematic representation of the circulation of the Ter River water in the lacustrine section of the Sau Reservoir. The intrusion depth of the river was calculated following Armengol et al. (1999). See the Methods section for the calculation of the depth of the seasonal thermocline.

The quantities measured were also expressed as flow-normalized loads or concentrations (for river constituents) and volume-normalized concentrations (for in-lake constituents), using:

$$Normalized\ load_i = \frac{Actual\ quantity_i}{Q_i} Q' \quad (2.1)$$

$$Norm.\ concentration_i = \frac{Actual\ quantity_i}{V'} V_i \quad (2.2)$$

where $Actual\ quantity_i$ is the measured load or concentration in time i, Q_i and V_i are the flow and volume in time i, and Q' and V' are the mean flow and volume for the whole period considered. Flow and volume normalisation eliminates the effect of the varying hydrology in the time-series (Stålnacke et al. 1999).

Due to the characteristics of our database, and in consonance with the Rigler's *recognition of the possible* (Rigler 1982), we did not try to develop a deductive, process-based model for the hypolimnetic biogeochemistry. Instead, we used the calculated volume-weighted summer averages and loads, and the other variables detailed above to explore linear relationships between all the variables, with the hope that this empirical regression approach would help to explain the main processes driving hypolimnetic nutrient chemistry. Although the significant correlations found by this analysis can be only regarded as empirical relationships or predictions in the sense of Rigler and Peters (1995), we inferred causal explanations supported by two facts. First, we worked in a single system with a seasonal time step. Thus, we avoided limitations that usually affect regressions including annual data for several systems, which necessarily lump a considerable number of processes. And second, we carefully examined alternative correlations and explanations to avoid formulating conclusions from spurious or indirect relationships.

Table 2.2 – Analytical methods used to characterize Ter River and Sau Reservoir water samples.

Determination	Analytical method
TN, TP	Grasshoff et al. (1983)
Nitrate	Liquid chromatography (Konik KNK 500-A)
Ammonia	Solorzano (1969)
Soluble reactive phosphorous	Murphy and Riley (1962)
DOC	Combustion in total carbon analyser provided with infrared sensor (Shimadzu TOC-5000)
Chl-a	Trichromatic method (Jeffrey and Humphrey 1975)

2.3 Results

2.3.1 The temporal development of the river load to Sau Reservoir

The Ter River has experienced a profound time-varying human impact during the last forty years, like many other rivers located in developed countries (Alexander et al. 2000). Marcé et al. (2004) showed that the nutrient load to Sau Reservoir rose dramatically until the early 1990s, to partially recover during the last decade, as remediation measures were implemented in the basin. This has been a common pattern for many polluted rivers located in populated areas (e.g. CERN 2000).

Remarkably, the study period includes almost all the annual inflow range found in the whole history of Sau Reservoir (Armengol et al. 1991). The series contains the driest year (1998), and the third wettest record (1996), only marginally inferior (12%) than the observed maximum, occurred in 1972 (Fig. 2.4). Thus, both very wet years and dry periods are lumped in subsequent analyses. This is a very important point, because hydrology is usually taken as a main driver in shaping reservoir processes in the Mediterranean region (Geraldes and Boavida 2004), where inter-annual variability of inflows is large.

The time evolution of TN and TP loads shows disparate patterns (Fig. 2.4B and C). TP did not follow any clear trend, with values ranging from 50 to 100×10^6 $g\ P\ yr^{-1}$. By contrast, the flow normalized TN load showed a sharp decrease during the late 1990s, maintaining values around 1.5×10^9 $g\ N\ yr^{-1}$ from 2001 to the present. The different behaviour showed by TN and TP load is due to the different timing of implementation of conventional WWTP and additional biological treatments. Whereas conventional treatments are efficient sequestering phosphorus from the effluent, the nitrogen compounds are only efficiently removed by biological treatments (Tchobanoglous et al. 2003). The effect of the WWTP on the TP load was apparent just after the WWTP were built during the early 1990s (*see* Marcé et al. 2004), but not afterwards (Fig. 2.4c). This indicated that most of the TP load currently comes from non-point sources, a conclusion also reached by Marcé et al. (2004) using a neuro-fuzzy regression modelling approach. By contrast, the TN load rapidly reacted to the implementation of biological treatments in the WWTP on the watershed both quantitatively and qualitatively. Whereas the nitrate load rose during the latter years, the ammonia load showed a two-fold decrease (Fig. 2.5A and B). In terms of the $NH_4^+ : NO_3^-$ molar ratio, these opposite trends are equivalent to a reduction from ca 2.5 to ca 0.1 (Fig. 2.5C).

The evolution of the flow-normalized DOC followed a pattern close to that shown for the TN (Fig. 2.4D). At the beginning of the period ca 2×10^9 $g\ C$ entered each year in the reservoir, contrasting with the ca 1.2×10^9 $g\ C\ yr^{-1}$ calculated for the last years. Like nitrogen, the organic matter is efficiently removed from effluents of biological WWTP (Tchobanoglous et al. 2003), therefore the DOC load reduction most probably reflects the implemen-

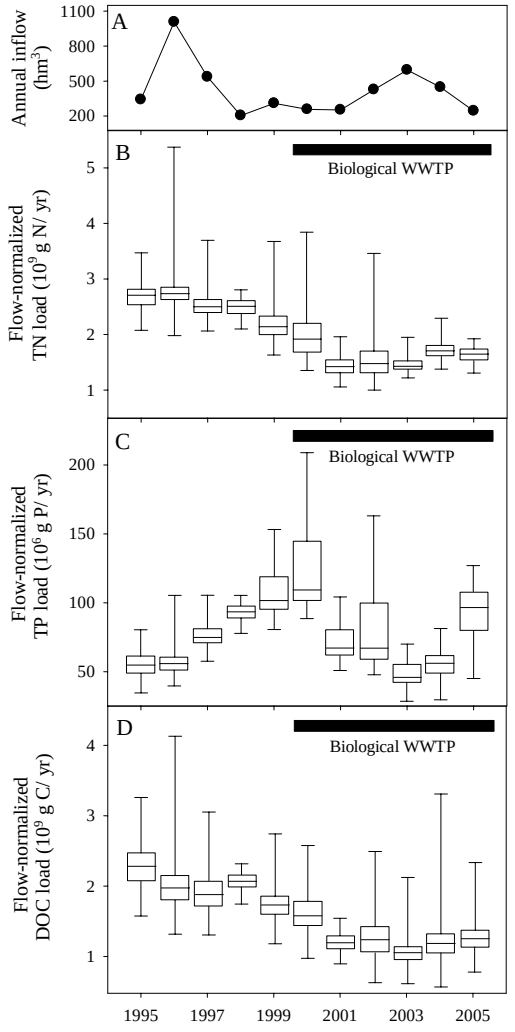

Figure 2.4 – (A) Annual water inflow to Sau Reservoir from the Ter River, and box-whisker plots for the calculation of the flow-normalized TN (B), TP (C), and DOC (C) load to the reservoir (middle line, median; lower box line, first quartile; upper box line, third quartile; lower whisker line, 2.5 percentile; upper whisker line, 97.5 percentile). Black bars mark the period with biological treatments in the WWTP of the basin.

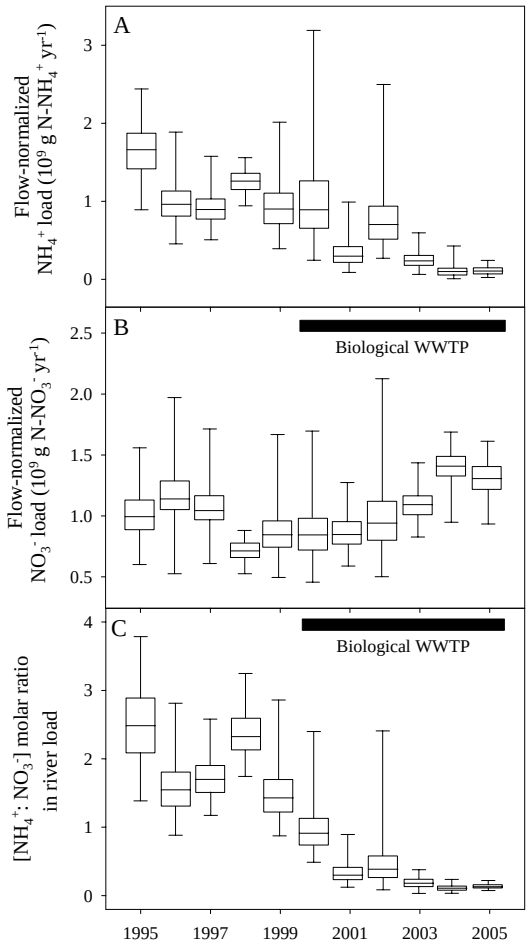

Figure 2.5 – Box-whisker plots for the calculation of the flow-normalized ammonia (A) and nitrate (B) load to the reservoir. (C) Box-whisker plots for the ammonia:nitrate molar ratio in river load during the studied period (middle line, median; lower box line, first quartile; upper box line, third quartile; lower whisker line, 2.5 percentile; upper whisker line, 97.5 percentile). Black bars mark the period with biological treatments in the WWTP of the basin.

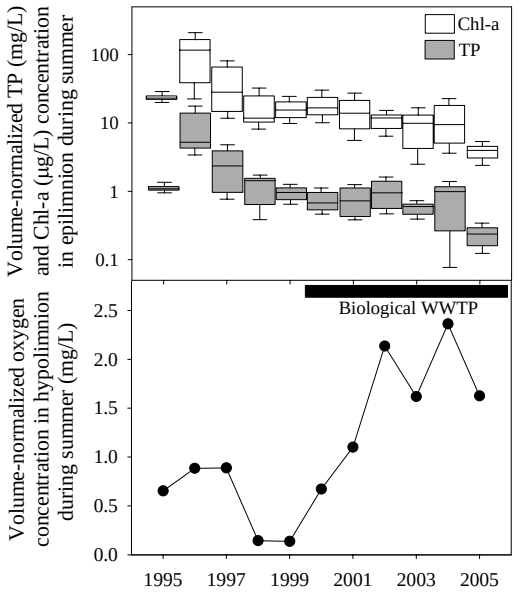

Figure 2.6 – (A) Evolution of the volume-normalized *PT* and *Chl-a* concentration in the summer epilimnion of Sau Reservoir (middle line, median; lower box line, first quartile; upper box line, third quartile; lower whisker line, 2.5 percentile; upper whisker line, 97.5 percentile). (B) Mean volume-normalized oxygen concentration in the summer hypolimnion of Sau Reservoir. Black bar marks the period with biological treatments in the WWTP of the basin.

tation of biological treatments in the watershed.

The reservoir response to these changes in the quantity and quality of materials incoming from the Ter River was not intuitive. The summer epilimnetic *Chl-a* and TP concentration showed a slight decrease (Fig. 2.6), although huge annual variability was present. On the other hand, the summer hypolimnetic oxygen content, expressed as the volume-normalized oxygen concentration, increased two-fold (Fig. 2.6).

2.3.2 Hypolimnion chemistry influenced by the river

The linear correlation analyses computed between the summer hypolimnetic oxygen concentration and a set of key variables measured both in the epilimnion and in the Ter River during summer (hereafter labelled with *epi* and *inflow* subscripts, respectively), showed that the only variables showing a significant impact (i.e. p-value $<$ 0.001) on the oxygen content in the hypolimnion were the DOC_{inflow}, TN_{inflow}, and $NO_{3\ inflow}^{-}$ (Table 2.3). Since any epilimnetic production proxy or hydrological variable accounted for the change in the observed hypolimnetic oxygen concentration (DOC_{inflow}, TN_{inflow}, and $NO_{3\ inflow}^{-}$ are not significantly correlated with the summer inflow), the classical assumption that the productivity of upper layers controls the hypolimnetic oxygen content is not valid in Sau Reservoir. Considering that the epilimnetic algal biomass does not explain oxygen variation, we must consider that the variability of other materials susceptible to be oxidized must account for the variation in the oxygen content.

Following the previous reasoning, an inverse and

Table 2.3 – Results of correlations between volume-normalized oxygen concentrations observed in the hypolimnion of Sau Reservoir during summer against a set of selected key variables measured in the epilimnion of the reservoir and the Ter River (also during the summer period).

	n	Pearson´s r	p-value
Summer inflow	11	-0.050	0.884
TP_{epi}	11	-0.218	0.519
SRP_{epi}	11	-0.258	0.443
TN_{epi}	11	-0.205	0.545
$NO_3^-{}_{epi}$	11	-0.118	0.729
DOC_{epi}	10	-0.083	0.819
Chl-a_{epi}	11	-0.195	0.564
TP_{inflow}	11	-0.375	0.357
SRP_{inflow}	11	-0.378	0.252
TN_{inflow}	11	-0.912	<0.001
$NO_3^-{}_{inflow}$	11	0.897	<0.001
DOC_{inflow}	11	-0.866	<0.001

statistically significant relationship between summer DOC_{inflow} concentration and the oxygen content in the hypolimnion (Table 2.3, Fig. 2.7) suggest that these may be linked mechanisitically. It is worthy to mention that the hypolimnetic *DOC* and the oxygen concentrations are non-correlated ($n = 10$, p-value $= 0.90$), therefore suggesting that the in-lake *DOC* concentration is not a good proxy for the *DOC* external input, at least at a seasonal scale. By contrast, the significant correlations between TN_{inflow}, $NO_{3\ inflow}^{-}$, and the oxygen content are not considered causal. The TN_{inflow} and DOC_{inflow} were strongly correlated (n=11, p-value < 0.0001), as were $NO_{3\ inflow}^{-}$ and DOC_{inflow} (n=11, p-value = 0.002). This is expected from the normalized load series depicted in Figures 2.4 and 2.5, which are the result of the implementation of biological WWTP in the watershed since 1995. Since more than 80% of TN_{inflow} were dissolved inorganic forms (*DIN*), the correlation between *DOC* load and *TN* load could not be attributed to the reduction of dissolved organic compounds in the river. Moreover, using $TN - DIN$ as a crude approximation of the organic nitrogen in the river, we did not find a significant correlation between organic nitrogen and the hypolimnetic oxygen content (n=11, p-value = 0.36). Since most of the initial NH_4^+ load is now oxidized in the WWTP before entering the river, the NO_3^- load rose promoting the strong correlation found between $NO_{3\ inflow}^{-}$ and DOC_{inflow}. Since no plausible mechanism could explain the control of the hypolimnetic oxygen by the nitrate or *TN* inflow coming from the river, and these variables are strongly correlated with DOC_{inflow}, we deduced that it was the progressive implementation of biological WWTP that caused the spurious covariance between inorganic nitrogen forms and oxygen in the hypolimnion.

Nevertheless, the river *DOC* input indirectly affects other features of the hypolimnetic chemistry through the control of the oxygen content. Concerning the phosphorous concentration, the *TP* summer hypolimnetic mean concentration (TP_{hypo}, $\mu mol\ P\ L^{-1}$) showed dependency on the surface area of anoxic sediment (SAS, m^2) during summer and nitrate concentration ($NO_{3\ hypo}^{-}$, $\mu mol\ N\text{-}NO_3^-\ L^{-1}$) in the hypolimnion ($n$=11, p-value = 0.001, R^2= 0.81):

$$TP_{hypo} = 3.27 + 8.7 \times 10^{-7}\ SAS - 0.015\ NO_{3\ hypo}^{-} \quad (2.3)$$

Independent variables were significant (p-value < 0.05) and not correlated ($n = 11$, p-value $= 0.32$, $r^2 = 0.11$). The combination of SAS (Fig. 2.8B) and $NO_{3\ hypo}^{-}$ (Fig. 2.8D) in the equation suggests that internal load processes linked to anoxic conditions and low redox potentials (inhibited by the presence of $NO_{3\ hypo}^{-}$) controls phosphorus dynamics. The relationship between DOC_{inflow} and *SAS* is dependent on the hypolimnetic volume. Thus, a significant positive correlation was found between DOC_{inflow} and the volume-normalized *SAS* (Fig. 2.8A). Moreover, the influence of the river on TP_{hypo} was also apparent through the relationship between $NO_{3\ inflow}^{-}$ and the volume-normalized summer nitrate concentration in the hypolimnion (Fig. 2.8C).

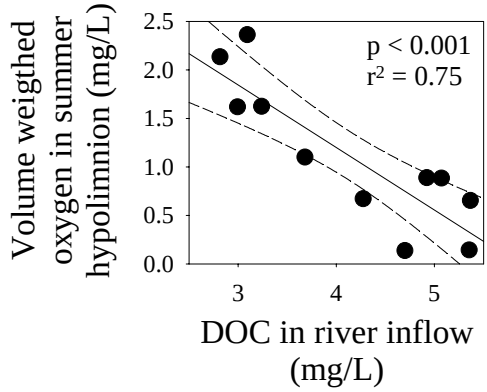

Figure 2.7 – Volume-normalized oxygen concentration observed in the hypolimnion of Sau Reservoir in summer against *DOC* concentration in the river inflow during summer.

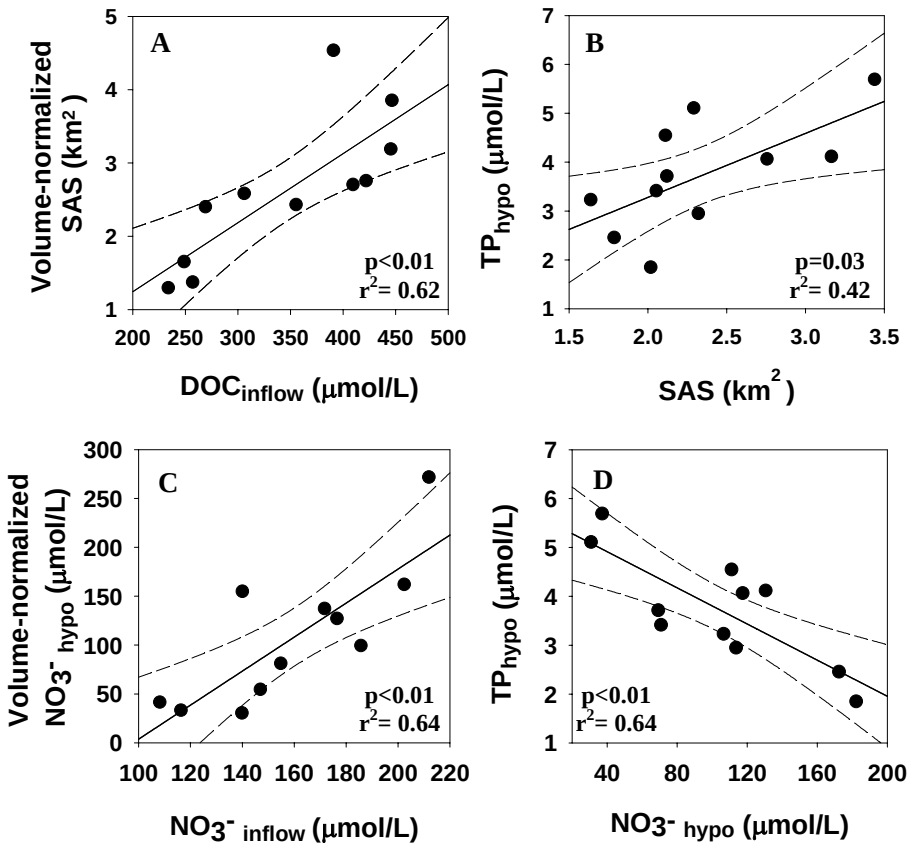

Figure 2.8 – The relationship between (A) DOC_{inflow} and the volume-normalized SAS, (B) SAS and TP_{hypo}, (C) $NO_{3\ inflow}^{-}$ and the volume-normalized $NO_{3\ hypo}^{-}$, and (D) $NO_{3\ hypo}^{-}$ and TP_{hypo}.

2.4 Discussion and Conclusions

In spite of the traditional scope focusing on the indirect effect in the hypolimnion biogeochemistry through epilimnetic processes, the hypolimnetic oxidation state in Sau Reservoir depends on a large extent on the quality of the water supplied by the Ter River. The reduction of the river *DOC* load curtailed the reducing power of hypolimnetic waters, thus decreasing the oxygen consumption in this layer and inhibiting the internal load of phosphorus. On the other hand, the enhanced nitrate load provides a high redox potential supplying resources for the denitrifying bacteria, which inhibits other energetically less-efficient reactions that deliver reduced compounds to the water. These two facts combined to improve the quality of the water stored in the hypolimnion, specially taking into account that during summer the river water directly plunges into this layer.

The application of nitrate as a redox buffer (i.e. an electron acceptor to improve the hypolimnetic redox potential) is an accepted procedure to manage thermally stratified eutrophic lakes and reservoirs by controlling the phosphorous release from sediments into overlying water (Ripl 1976, Foy 1986, Boström et al. 1988, Erlandsen et al. 1988, McAuliffe et al. 1998; Lucassen et al. 2004; Wauer et al. 2005). Nitrate is easily dissolved in lake water and its solubility is orders of magnitude higher than that of oxygen. It deeply penetrates into the sediment and creates a large pool of oxidized iron (Hansen et al. 2003), which retains phosphorous in surface sediments (Jensen and Andersen 1992). Moreover, Ripl (1978) suggested the deep-water injection of nitrate rich effluents from advanced wastewater treatment plants to enhance sediment phosphorous binding and increase the hypolimnetic redox potential (Cooke et al. 1993). In the case of Sau Reservoir, the Ter River directly introduces nitrate into the deep layers of the water column during the stratification period, thus proceeding like a natural nitrate bioremediation measure. Nevertheless, this beneficial effect should be considered in the context of a phosphorus limited environment like Sau Reservoir (Nedoma et al. 2006). Obviously, in a nitrate limited water body the validity of the above conclusion would be dubious.

It is generally accepted that control of nutrient inputs is a crucial factor in restoring aquatic ecosystems from cultural eutrophication. Diversion and advanced wastewater treatment constitute the two most usual techniques to reduce external loading. Diversion of treated sewage or industrial wastewater involves the construction of interceptor lines to drive the polluted inflow away from the degraded waterbody. However, even though removing a significant fraction of external loading, this methodology does not always result in the expected trophic level reduction and ecosystem improvement. Based on accounts of some 57 world lakes to which nutrient inputs were reduced, Cooke et al. (1993) pointed out that the response of lakes to external load reduction was generally slow and/or less intense than expected. In this context, Scharf (1999) and Luglié et al. (2001) reported the failure of the attempt to recover highly eutrophic reservoirs by nutrient diversion. In both cases, the reduction of in-lake TP and *Chl-a* concentration was insufficient to change the reservoir trophic category, even 10 years after the urban and industrial wastewater diversion. Additionally, Kleeberg and Kozerki (1997) showed that the consequence of the reduced supply of nitrate to Lake Müggelsee was an enhanced phosphorous release from sediments and the loss of phosphorous retention, this internal loading counteracting the decreasing external phosphorous load as a prime aim of lake restoration practice. Thus, in many cases (especially when internal loading of nutrients is significant) the declines in nitrate concentration due to external input diversion may result in electron acceptor depletion and increases in the release of phosphorous from the sediments to the water column, so nutrient diversion seems to be an ineffective technique for eutrophic systems if not accompanied by in-lake costly internal load control measures (Björk 1972; 1974; Cooke et al. 1978).

A very different scenario results when biological WWTP are built in the watershed flowing treated waters upstream the reservoir. As our results have

demonstrated, their implementation not only dramatically reduce nutrient and organic matter loads to the waterbody, but it also induce a qualitatively change in the inflowing water. In the case of Sau Reservoir, biological WWTP diminished the *DOC*, phosphorous and ammonia loads to the reservoir while nitrate showed an increasing trend thus controlling the phosphorous internal load dynamics. This control effect results especially intense in advectively dominated reservoirs, where the inflow water directly plunges into the hypolimnion during summer. It is worth to note that if the water outlet of the reservoir is located below the level of the seasonal thermocline, this additional flushing of nutrients through the outlet will also contribute to maintaining the hypolimnion with a reasonably good water quality. All these strategies combined have resulted in a low-cost and highly efficient control of the eutrophication process in Sau.

We can conclude that in canyon-type reservoirs, where the river water typically enters directly into the hypolimnion via a density current, the dynamics of this deep layer is directly forced via a driver that is essentially independent of in-lake processes. Although some previous studies have considered the role of river inflow on reservoir dynamics (e.g. Knowlton and Jones 1989) this important point has been frequently forgotten in reservoir water quality assessment, where the management of anoxia and its deleterious effects on water quality is an old concern. In any case, successful system-broad remediation measurements should take into account nutrient and organic matter reduction programmes combined with concomitant inflow quality changes. The results presented here should prompt reservoir limnologists to always take into account the probable effect of allochthonous sources in the hypolimnetic oxygen content and nutrient dynamics, especially in human-impacted systems.

Chapter 3

The role of allochthonous inputs of dissolved organic carbon on the hypolimnetic oxygen content of reservoirs

3.1 Introduction

Ecologists have long recognized that lacustrine ecosystems are open systems, especially after the seminal work by Vollenweider (1968), in which the principal role of the external nutrient loading in the eutrophication of surface waters was first systematically explored. Later, the prevalence of phosphorus as the limiting factor for primary production was fully demonstrated (Schindler 1977), founding the basis for a classical topic in ecosystem empirical modeling (Chapra 1997). The prediction of epilimnetic producers biomass by means of empirical relationships with allochthonous phosphorus is still in use, although some refinements have been developed, including into equations internal loading terms, trophic cascade effects, or organic matter interactions with the light climate (e.g. Beisner et al. 2003).

By contrast, the summer hypolimnion of lakes and reservoirs, although being part of a larger open system, is often considered isolated from direct interactions with the atmosphere and tributaries. In this context, the external drivers can only reach this layer indirectly, through exchanges with the epilimnion, or through interactions with the sediments, that in fact are usually modeled as a function of epilimnetic variables (e.g. Carpenter et al. 1999). Thus, hypolimnetic quantities or processes like oxygen content or phosphorus internal loading have usually been modeled as a function of variables measured at the epilimnion, or that are supposed to drive epilimnetic processes (Reckhow and Chapra 1983; Nürnberg 1984; Nürnberg 1995; Livingston and Imboden 1996).

For most natural lakes from the temperate and subtropical regions, the assumption that the summer hypolimnion is isolated from direct atmospheric or tributaries interactions appears to be an acceptable simplification. These systems develop a well-

defined thermocline that precludes direct exchanges between deep layers and the atmosphere (Wetzel 2001), and the runoff penetration into the hypolimnion is small and dispersive (Wetzel 1990). However, man-made mainstream reservoirs show a relatively high drainage basin area: water body area (BA:WA) ratio (Straškraba 1998), implying a strong advective flux from the river tributaries even during the low-flow summer conditions. This promotes the recurrent presence of the river water as density currents in the reservoir (Ford 1990), which can plunge into the hypolimnion. In such a scenario, the assumption that the hypolimnion is isolated from the direct influence of the river inflow would not be correct.

The empirical modeling of the oxygen content or oxygen deficit in the hypolimnion of water bodies is a good example of a hypolimnetic quantity modeled as a function of epilimnetic processes. Although both lake morphometry and hydrology are usually present in the empirical equations, the phytoplankton biomass, which is supposed to eventually sink and decay in the deep layers, always has a significant role. The epilimnetic productivity can be incorporated into equations using different proxies, including photosynthetic pigments concentration (Charlton 1980), in-lake phosphorus content (Cornett and Rigler 1980; Molot et al. 1992), phosphorus retention (Cornett and Rigler 1979; Cornett 1989), or the phosphorus river content (Reckhow 1979; Nürnberg 1995). However, with the exception of brown-water lakes (Hutchinson 1957; Houser et al. 2003), and lakes receiving significant humic and fulvic acids inputs (Nürnberg 1995), no significant role on the hypolimnetic oxygen consumption has typically been assigned to the input of allochthonous oxidable substances. Lately, some studies have pointed out the importance of allochthonous organic mater in the oxygen consumption and global metabolism of oligotrophic lakes (del Giorgio et al. 1999; McManus et al. 2003; Pace and Prairie 2005), and bacterial growth (Jansson et al. 2003; Kritzberg et al. 2004), therefore indicating that the classical nutrient load-response model assumptions could not be applicable to a considerable number of lakes. In despite of this, empirical hypolimnetic oxygen equations based exclusively on morpho-hydrological features and primary productivity are still in use, although the significance test for the effect of the productivity proxy fails even in very productive systems (e.g. Nürnberg 2002).

In this work we show that assumptions of classical models concerning the oxygen content in the hypolimnion do not necessarily hold in reservoirs, in the sense that the organic matter entering the hypolimnion from the river inflow could have a principal role. Following McManus et al. (2003) and Biddanda and Cotner (2002), who found that dissolved organic carbon (*DOC*) from allochthonous sources plays a significant role on the carbon cycling in lakes Superior and Michigan, our hypothesis was that allochthonous *DOC* could exert a significant effect on the hypolimnetic oxygen content even in very productive systems if the *DOC* input is high enough. In the case of reservoirs, the effect of external inputs of *DOC* on the hypolimnetic oxygen content should be enhanced by the fact that density currents can directly inject allochthonous materials into the bottom layers. Thus, the *DOC* input do not enter in the epilimnetic food web, which can mask its role in the subsequent hypolimnetic oxygen depletion caused by sedimentation of epilimnetic organic matter. In addition, the lability of allochthonous *DOC* could be a critical feature to explain the hypolimnetic oxygen content in reservoirs, because these systems tend to show relatively short water residence time. Since *DOC* lability characterization is not frequent in databases, we previously explored the adequacy of chloride concentration (much more frequent in databases) as a proxy of labile *DOC* in reservoir tributaries included in this study. Then, main results are presented in two steps. First, we tested the role of alochthonous *DOC* on the hypolimnetic oxygen content using long-term data from two reservoirs receiving a relatively high *DOC* input of human origin. Both, an empirical regression approach and a more deductive analysis were used here. Finally, we examined the implications of our results for the empirical modeling of hypolimnetic reservoir anoxia, applying the Nürnberg's (1995) seminal approach on the anoxic factor (AF) to the former and two additional reservoirs

showing contrasted human impact.

3.2 Materials and Methods

3.2.1 Study sites

Table 3.1 summarizes some limnological features of the four reservoirs included in this study. Sau and Foix reservoirs are located in populated areas in NE Spain near the city of Barcelona, and dam the Ter River and the Foix River, respectively. Brownlee (Snake River, Idaho) and Pueblo (Arkansas River, Colorado) reservoirs are located in low population density areas in the USA. This set of reservoirs covers very small reservoirs (Foix) and large reservoirs draining vast areas (Brownlee). However, all of them have water retention time below one year, suggesting that the river input is relatively high respect their volume. This is not at odds with the high BA:WA ratio showed by the four reservoirs.

Considering chlorophyll *a* level (*Chl-a*, Table 3.1), trophic status ranges from mesotrophy (Pueblo Reservoir) to hypereutrophy (Foix Reservoir). The human impact in the eutrophication process of Sau (Vidal and Om 1993), Foix (Marcé et al. 2000), and Brownlee reservoirs (Freshwater Research and Brown & Caldwell 2001; IDEQ and ODEQ 2004) is well documented. Pueblo Reservoir drains a mountainous region where the human impact seems to be comparatively less important (Crowfoot et al. 2003). The average *DOC* concentration in the river tributaries (Table 3.1) ranges from 2.5 $mg\ C\ L^{-1}$ (Arkansas River) to 6.3 $mg\ C\ L^{-1}$ (Foix River), but few information is available about the bioreactivity of *DOC* in these rivers. However, in Sau Reservoir empirical evidence suggest that most part of the incoming river *DOC* is labile, coming mainly from urban, industrial, and farming spills that accumulate upstream the reservoir (Romaní and Sabater 1999). By contrast, the labile fraction in the Snake River upstream Brownlee Reservoir seems to be a small percentage of the total *DOC* (Harrison 2005).

3.2.2 Chloride as a proxy of labile *DOC*

One of the main impacts of urban areas and farming activities on river water quality is the loading of labile organic substances to the watercourses (Viessman and Hammer 1993; Søndergaard and Middelboe 1995; Westerhoff and Anning 2000; Tchobanoglous et al. 2003). Since these human activities are usually associated to inputs of chloride (Daniel et al. 2002), we can use chloride concentration as a proxy of the relative impact of these human activities on rivers. However, to use chloride as a tracer of relative human impact in a river other potential sources of chloride (mainly weathering and atmospheric inputs) must be quantified. None of the four watersheds considered in this study have significant geological sources of chloride (*see* Whittemore [2000] for Pueblo watershed; ICC [2002] for Sau and Foix watersheds; and Bond [1978] for Brownlee watershed). Thus, we neglected the role of geology as a source of this ion. On the other hand, the average river chloride concentration is much higher than the mean chloride concentration measured in rain falling on the watersheds drained by these rivers (Table 3.1). However, chloride concentration in a river free of human related spills ($Cl^-_{PRISTINE}$) could be much higher than chloride concentration in rain, because evapotranspiration concentrates this ion in soils (Lovett et al. 2005). Thus, we calculated a crude estimation of $Cl^-_{PRISTINE}$ (Table 3.1) as the quotient between mean chloride concentration in rain and the annual runoff coefficient (i.e., the fraction of precipitation that is eventually delivered as effective runoff to rivers). Since water residence time in soils is usually greater than one year (Michel 1992), and chloride is not a true conservative ion in watersheds (Lovett et al. 2005), reported $Cl^-_{PRISTINE}$ estimates in Table 3.1 should be considered as order-of-magnitude annual mean expectations. Since no geological sources are supposed, observed river chloride concentrations much higher than $Cl^-_{PRISTINE}$ (especially in Sau and Foix reservoirs tributaries, Table 3.1) must be attributed to human activities (i.e., urban, industrial, and farming activities). De-

Table 3.1 – Selected limnological features of the four reservoirs and tributaries included in this study. For some magnitudes standard deviation are given in brackets.

	Sau [a]	**Foix** [b]	**Brownlee** [c]	**Pueblo** [d]
Maximum volume (hm^3)	168.5	5.6	1533	650.8
Maximum area (WA, km^2)	5.8	0.72	47.5	32.3
Maximum depth (m)	65	10	85	52
Mean depth (m)	25.2	7	32.3	21
Maximum length (km)	18	4	80	6
Maximum width (km)	1.3	0.25	0.9	1.5
Mean inflow ($hm^3\ yr^{-1}$)	540.5	19.3	15632	713.4
Mean residence time (yr)	0.31	0.29	0.08	0.91
Basin area (BA, km^2)	1380	289	189000	23906
BA:WA ratio	238	401	3981	740
Mean *Chl-a* in epilimnion ($\mu g\ L^{-1}$)	9.6	95.8	7.0 [e]	3.9
DOC in river inflow ($mg\ L^{-1}$)	4.1 (2.3)	6.3 (1.4)	4.5 (3.1)	2.5 (0.4)
C:N ratio in river organic matter	8.3 (6.5)	3.1 (2.4)	12.5 (14.0)	17.8 (12.1)
Chloride in river inflow ($mg\ L^{-1}$)	94.9 (53.2)	238.6 (107.4)	19.7 (5.5)	8.2 (3.5)
$Cl^-_{PRISTINE}$ in river inflow ($mg\ L^{-1}$)	3.17 [f]	25.86 [g]	3.48	4.52
Mean chloride in rain ($mg\ L^{-1}$)	1.01 [h]	1.90 [i]	0.68 [j]	0.35 [k]
Annual watershed runoff coefficient [l]	0.32	0.07	0.20	0.08

[a] Chemistry data from Joan Armengol (*Unpublished Data*). For DOC data $n = 129$, for chloride data $n = 132$, and for C:N ratio $n = 103$.
[b] Chemistry data from Joan Armengol (*Unpublished Data*). For DOC data $n = 21$, for chloride data $n = 27$, and for C:N ratio $n = 12$.
[c] Chemistry data from USGS-NWIS database. For DOC data $n = 171$, for chloride data $n = 166$, and for C:N ratio $n = 124$.
[d] Chemistry data from USGS-NWIS database. For DOC data $n = 23$, for chloride data $n = 181$, and for C:N ratio $n = 8$.
[e] Freshwater Research and Brown & Caldwell (2001). Data are for Site 5 in this report.
[f] Coincides reasonably well with mean chloride concentrations measured in pristine streams near the sampling point (4 to 7 $mg\ L^{-1}$, Butturini [1998]).
[g] Very similar to mean chloride concentration measured in pristine streams of the same typology in the area (17 to 28 $mg\ L^{-1}$, Bernal [2006]).
[h] Avila and Alarcon (1999).
[i] Alcalá (2005).
[j] James P. McNamara (Unpublished Data).
[k] Claassen and Halm (1995).
[l] Computed using long term means of precipitation falling on the watershed and the streamflow series.

icing salt road application are not considered relevant for this study, because the chemical effects of road runoff on surface water ecosystems are usually confined to small streams (Forman and Alexander 1998) and highly urbanized watersheds (Kaushal et al. 2005), and salt road application in the Spanish watersheds considered in this study is very unusual.

Following the previous reasoning and values in Table 3.1, we can use the chloride concentration in the river inflows as an estimate of the relative impact of urban areas and farming activities. By extension, this will also work as a rough but useful tracer of the origin of the *DOC* content of these rivers. In this context, low *DOC* content in the Arkansas River upstream Pueblo Reservoir seems to be mainly associated to terrestrial, low reactive sources; while most *DOC* upstream Sau and Foix reservoirs are probably labile *DOC* coming from human activities. By contrast, high *DOC* values in the Snake River coincided with relatively low chloride concentrations, suggesting again that most of the *DOC* carried by the Snake River is not of human origin, but coming from terrestrial ecosystems.

The above interpretations are also supported by an analysis of the $C:N$ atomic ratio of the organic matter (Table 3.1) and its relationship with river chloride concentration (Figure 3.1). $C:N$ values above 15 indicate strong influence of organic matter coming from terrestrial ecosystems (Kendall et al. 2001; McKnight et al. 2003), while values below 4 are exceptional (Kendall et al. 2001), and should be attributed to the influence of spills loaded with nitrogen rich organic compounds like urine or slurries (Werner et al. 1989). High N content in the organic matter also is a good indicator of organic carbon bioavailability (Benner 2003). Thus, an inverse relationship is expected between $C:N$ ratio and the relative influence of human activities on the river. Figure 3.1 summarizes this relationship for the four rivers considered, using chloride concentration as a proxy of the relative impact of human activities. Since $C:N$ ratios are affected by in-stream processes and several natural and anthropogenic sources (Findlay and Sinsabaugh 2003), the relationship using instantaneous data (Figure 3.1A) shows substantial scatter. However, as we lump data

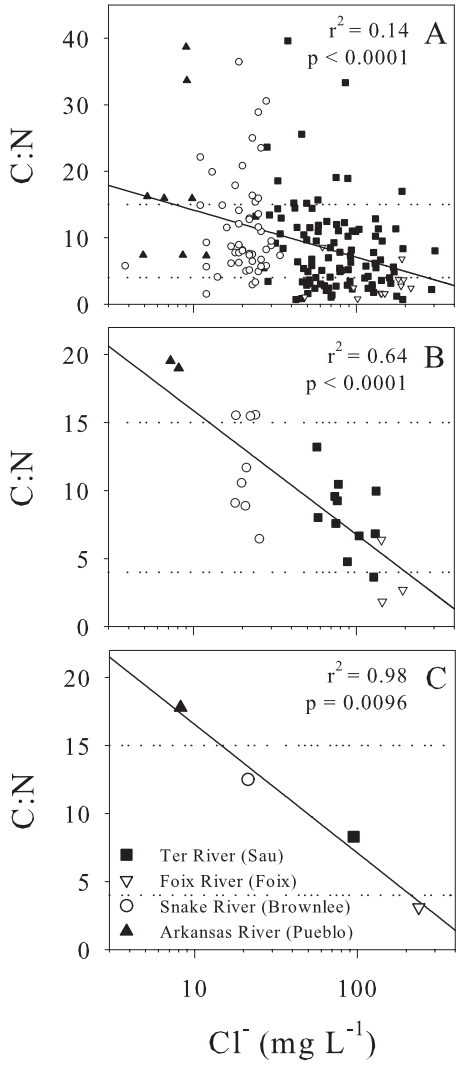

Figure 3.1 – $C:N$ ratio in organic matter against chloride concentration in the river tributaries of the four reservoirs included in this study. The significance and explained variance for a logarithmic relationship using (A) instantaneous data, (B) annual averages, and (C) long term averages are detailed. Panel (B) only includes years with at least three data pairs to calculate the annual mean. Dotted horizontals lines at $C:N = 15$ and $C:N = 4$ are plotted for reference. Data for Ter and Foix rivers (Joan Armengol, *Unpublished Data*) come from elemental analyses. Data for Snake and Arkansas rivers comes from the USGS-NWIS database.

into longer time periods, e.g. annual or long term means (Figures 3.1B and C), the influence of human activities on the $C:N$ ratio is much more crisp. Last but not least, $\delta^{13}C$ values measured in the particulate matter upstream Sau Reservoir during year 2000 (Rafael Marcé, *Unpublished Data*) ranged between -23.90 and -18.05 ‰, which are substantially higher than typical values for rivers (Kendall et al. 2001; Raymond and Bauer 2001; McCallister et al. 2004). This also suggests the presence of a supplementary organic carbon source not related to terrestrial ecosystems.

All in all, the four systems included in this study can be placed in a gradient of increasing relative human impact, and of lability of organic matter coming from tributaries. In this ordination, Foix Reservoir suffers the strongest human impact, and receives most *DOC* load in labile, nitrogen rich forms. In the opposite side, Pueblo Reservoir undergoes a relative low human impact, and receives organic carbon in low reactive forms.

3.2.3 Data collection

Data for Sau and Foix reservoirs and its tributaries showed throughout this paper comes from water quality monitoring programs led by the authors. In Sau Reservoir monitoring started in 1995 and this work includes data until 2005. Sampling was monthly, consisting in surface to bottom 1 m resolution vertical profiles of temperature, pH, conductivity, and oxygen concentration collected with a multiparametric probe (TURO T-611). The sampling station was located at the lacustrine section of the reservoir. Based on these profiles, a variable number of water samples were collected with a 5 L hydrographic bottle (UWITEC), in order to accurately describe the vertical heterogeneity in the sampling point. The samples were stored in dark bottles and immediately processed in a nearby laboratory. Samples were analyzed for total nitrogen (TN) and total phosphorus (TP) following Grasshoff et al. (1983); for soluble reactive phosphorus (*SRP*) by colorimetric (Murphy and Riley 1962); for *DOC* in a total carbon analyzer (Shimadzu TOC-5000); for chloride (Cl^-) by liquid chromatography (Konik KNK 500-A); and for *Chl-a* with the trichromatic method (Jeffrey and Humphrey 1975). The sampling at the river location was identical, but consisting only on one integrated water sample collected just upstream the reservoir. However, *Chl-a* analyses were not performed on river samples. Water leaving the reservoir through deep outlets was also sampled with the same periodicity. The government water agency (Agència Catalana de l'Aigua, ACA) supplied daily hydrological data.

The database for Foix Reservoir is less complete, starting during 1995 but lasting only until 2002, with a one-year gap at 2000. Sampling was more irregular, with bimonthly frequency during some periods. In addition, not all the variables mentioned above for Sau Reservoir were consistently measured throughout the monitoring program in Foix Reservoir, and conspicuous gaps are present for some variables. Lab analyses and field procedures were as detailed above for Sau Reservoir.

Data for the Snake River, and for Pueblo Reservoir and its tributary come from the United States Geological Survey National Information System (USGS-NWIS) database. Data for the Snake River were obtained from stations Snake River at Weiser (USGS-NWIS Station Number 13269000), and Snake River near Murphy (USGS-NWIS Station Number 13172500). Collected data included daily streamflow, river Cl^- concentration, and river *DOC* concentration. However, no useful data for this study collected at Brownlee Reservoir were found in the USGS-NWIS. Alternatively, reservoir data comes from Nürnberg (2002) and Freshwater Research and Brown & Caldwell (2001), consisting basically in calculations of the AF for seven years (1970, 1991, 1993, 1994, 1997, 1999, and 2000).

Daily streamflow, and river Cl^- and *DOC* concentration data for the Arkansas River upstream Pueblo Reservoir were collected at Arkansas River near Portland, CO (USGS-NWIS Station Number 07099200), and Arkansas River at Portland, CO (USGS-NWIS Station Number 07097000). AF's for 21 years (1985 to 2005) were calculated as detailed below using data from Pueblo Reservoir Site 7B (USGS-NWIS Station Number 381602104435200), including temperature and dis-

solved oxygen profiles.

3.2.4 Empirical regressions with hypolimnetic oxygen

As a first approximation to describe the driving mechanisms controlling oxygen dynamics in the hypolimnion, we calculated correlations between the summer hypolimnetic oxygen concentration and several quantities usually involved in empirical formulations of the oxygen content in lakes and reservoirs. We only used data from Sau and Foix reservoirs, because databases for Brownlee and Pueblo would not permit a comparable analysis.

The depth of the seasonal thermocline was estimated with the location of a density gradient of at least 0.15 $kg\ m^{-3}\ m^{-1}$, threshold that consistently avoided the daily thermocline or other transient structures. Then we calculated volume-weighted concentrations of the different constituents in the epilimnion and hypolimnion, averaging the values obtained between June and September to get mean summer values for each different year. For the epilimnion, mean spring concentrations (March to May) were also calculated. Since the volume of the reservoirs was highly variable between years, we expressed the variables measured in the hypolimnion and epilimnion as volume-normalized concentrations, to account for the variability in the volume stored in the reservoir (Stålnacke et al. 1999):

$$Normalized\ concentration_i = \frac{Actual\ concentration_i}{V'} V_i \qquad (3.1)$$

where $Actual\ concentration_i$ is the mean volume-weighted concentration during the period (summer or spring) of the i^{th} year, V_i is the volume of the hypolimnion or epilimnion during the period of the i^{th} year, and V' is the mean volume of the hypolimnion or epilimnion for the whole period (i.e, all the years in the database).

Mean summer concentrations for variables measured in the river tributaries were computed reconstructing daily concentration traces using the methodologies described in Marcé et al. (2004)[1], and averaging the values obtained between June and September.

Since most classical empirical approximations to the oxygen content in the hypolimnion take care of epilimnetic processes, we tested volume-normalized mean summer oxygen concentration in the hypolimnion (O_2^{hypo}) against six variables measured during summer in the epilimnion (TP_{epi}, SRP_{epi}, TN_{epi}, DOC_{epi}, Cl^-_{epi}, and $Chl\text{-}a_{epi}$). Since it can be argued that maximum epilimnetic biomass development in temperate water bodies is usually found during the spring, we also tested O_2^{hypo} against the mean epilimnetic concentrations calculated for the spring periods ($Spring\ TP_{epi}$, $Spring\ SRP_{epi}$, $Spring\ TN_{epi}$, $Spring\ DOC_{epi}$, $Spring\ Cl^-_{epi}$, and $Spring\ Chl\text{-}a_{epi}$). Finally, we calculated correlations between O_2^{hypo} and variables measured during summer in the river inflow (TP_{inflow}, SRP_{inflow}, TN_{inflow}, DOC_{inflow}, and Cl^-_{inflow}), and also with the mean water inflow to the reservoir during summer.

Correlations were tested using the Spearman's τ test (Sokal and Rolf 1995), because the number of available observations (maximum n=11) did not allow an accurate assessment of assumptions needed to apply parametric procedures. In addition, due to the large number of significance tests performed for each reservoir (i.e., 18), we recalculated the significance of all the previously significant results applying the sequential Bonferroni adjustment (Sokal and Rolf 1995). However, non-adjusted significance levels will also be given in this work for all tested correlations, for reasons that are best explained in Moran (2003).

3.2.5 Oxygen consumption in the hypolimnion as a first order process

The simple correlation analysis presented in the preceding section requires additional information in order to support potential conclusions drawn from this crude approximation. If the *DOC* content of

[1] Chapter 1 in this Thesis

the river entering the reservoir has to control the oxygen content of the hypolimnetic layer, a good agreement between the river *DOC* load and the oxygen consumption in the hypolimnion during a given period should exist. The rationale of this approach relies on the assumption that the decay of organic carbon is stoichiometrically linked to oxygen consumption. For oxic environments this is a reasonable assumption, since values of the respiratory quotient for most organic materials are close to one (Williams and del Giorgio 2005). However, if other metabolic pathways not involving oxygen as electron acceptor are important for the carbon cycling, the relationship between organic carbon decay and oxygen consumption could be masked. Moreover, two assumptions are required: that most of the river inflow directly enters the hypolimnion via a density current, and that hypolimnion and epilimnion have no major exchanges. Obviously, summertime is the best period to test such hypothesis.

We calculated the oxygen consumption in monthly or bimonthly periods during summer in Sau and Foix reservoirs. We accounted for the difference in the oxygen content of the hypolimnetic layer between the start and the end of the period ($\Delta O_{2hypo} = O_{2hypo\_initial} - O_{2hypo\_final}$), the oxygen load from the river inflow during the same period ($O_{2inflow}$), and the oxygen leaving the hypolimnion through deep outlets (O_{2out}):

$$Oxygen\ consumption\ (mol\ O_2\ period^{-1}) = \Delta O_{2hypo} + O_{2inflow} - O_{2out} \quad (3.2)$$

ΔO_{2hypo} was calculated from the vertical oxygen profiles and the volume of water stored in the hypolimnion. $O_{2inflow}$ was calculated from the daily water inflow and the oxygen data measured upstream the reservoir. O_{2out} was calculated interpolating the oxygen concentration measured in the water leaving the reservoir, to build a daily series that was combined with the daily outflow record. To guarantee that advective or turbulent exchanges between epilimnion and hypolimnion were not severely influencing this analysis, periods showing final oxygen concentration higher than the initial one were discarded, because increasing oxygen concentrations in the bottom layers could be the result of strong mixing with surface water. Noticeably, most discarded periods corresponded to the beginning or the end of the summer, when mixing episodes are more probable. We found 28 valid periods for Sau Reservoir, but only three valid periods could be extracted from the Foix Reservoir database.

The *DOC* load from the river inflow ($mol\ C\ period^{-1}$) was calculated following Marcé et al. (2004) from measured river *DOC* concentrations and the daily streamflow record. Finally, to assess whether the presence of the river inflow as a density current during summer was a valid assumption, we estimated the river insertion depth from the temperature profiles collected in the reservoirs, and the temperature measured in the rivers. Although some aspects of the river circulation in a lentic ecosystem are difficult to simplify, the depth of intrusion of river water in the reservoir can be reasonably well predicted assuming that the river inflow will plunge to the depth that minimizes the density differences between river and reservoir water (Armengol et al. 1999).

3.2.6 Anoxic Factor modeling

We also investigated the role of allochthonous organic matter on the year-to-year dynamics of one of the most extensively applied descriptors of the oxygen content in lakes and reservoirs. We revisited the empirical approaches used to predict the AF (Nürnberg 1995), explicitly including the allochthonous sources in the equations. In the seminal paper by Nürnberg (1995), the hypolimnetic oxygen content was described by means of a variable (AF, $days\ season^{-1}$) that accounts for the spatial and temporal extent of the anoxia, therefore comparable between systems or between periods in a single water body. AF is given by:

$$AF = \sum_{i=1}^{n} \frac{t_i \times a_i}{A_0} \quad (3.3)$$

where t_i stands for the period ($days$) of anoxia (i.e. water with less than 1 $mg\ O_2\ L^{-1}$), a_i the correspond-

ing anoxic area (m^2), A_0 the average surface lake or reservoir area during the period (m^2), and n is the number of periods with different oxycline depths. Since it was first proposed, the AF has been widely used as a tool for lake and reservoir management (Nürnberg 2002; Townsend 1999; Matthews et al. 2006), and as a descriptor of eutrophication trends in paleolimnological research (Quinlan et al. 1998; Reavie 2006).

In Sau, Foix, and Pueblo reservoirs the summer AF (June to September) was calculated from the oxygen profiles. The exact depth of the 1 $mg\ O_2\ L^{-1}$ isopleth was estimated by linear interpolation, and the corresponding area was calculated with reservoir-specific depth-area plots. Anoxic area values between sampling dates were linearly interpolated. For Brownlee Reservoir we used the AF values calculated in Nürnberg (2002).

Empirical regressions between the AF and variables usually involved in the prediction of this variable were then calculated. Since some measure of the hydrological behavior of the system is always considered in the equations (Townsend 1999; Nürnberg 2002), we included the mean summer inflow as a master independent variable. In addition, classical proxies of the primary production in the epilimnion (TP_{epi}, $Chl\text{-}a_{epi}$, $Spring\ TP_{epi}$, and $Spring\ Chl\text{-}a_{epi}$) were combined with the mean summer inflow in multiple regressions with two independent variables. Finally, DOC_{inflow} and Cl^{-}_{inflow} were also included as independent variables to assess the effect of the inflowing materials on the AF interannual variability. Due to limitations in the available data, regressions with the epilimnetic variables were only applied for AF's calculated for Sau and Foix reservoirs, and DOC_{inflow} could not be calculated in Brownlee Reservoir. For the same reason, some of the AF calculations could not be used because we could not calculate appropriate paired data from the river. Finally, since few cases were generally available to calculate regressions, the normality assumption could not be correctly assessed, although extreme outliers were not present in any variable. Consequently, all significance levels (for both the whole regression and the partial effects) were calculated with permutation tests (Anderson and Legendre 1999), using software by Legendre (2002).

3.3 Results

3.3.1 Allochthonous *DOC* and hypolimnetic O_2

Figure 3.2 summarizes the time evolution of streamflow, TP, TN, and DOC concentration in the main inflow of Sau and Foix reservoirs. Remarkably, the Sau Reservoir database includes almost all the annual inflow range found in the whole history of the reservoir (Armengol et al. 1991), and we also found a wide range in the streamflow measured in the Foix River. Thus, both very wet years and dry periods are lumped in subsequent analyses. This is a very important point, because hydrology in the Mediterranean region is highly variable, and this has profound effects on reservoir processes (Geraldes and Boavida 2004).

We can observe a clear trend in TN and DOC concentrations in the inflow to Sau Reservoir, which decreased by almost 50% during the eleven years period (Figure 3.2). This has been related to the implementation of biological treatments in the wastewater treatment plants of the watershed during the late 1990's (Marcé et al. 2006), because these treatments are efficient removing nitrogen compounds and organic matter from effluents. By contrast, TP concentration did not follow a clear trend, because very high river TP concentrations measured in the river were already lowered by the physicochemical treatments implemented during the late 1980's (Marcé et al. 2004). Time series for the Foix River are less complete, and it is difficult to establish temporal trends. However, it is worthy to mention the extremely high TN and TP concentrations found in this reservoir inflow.

The response of Sau and Foix reservoirs to these nutrient inputs was non-intuitive. In Sau Reservoir the classical proxies of the epilimnetic algal biomass (TP and $Chl\text{-}a$, Figure 3.3) did not respond to the temporal changes of nutrient inputs from the river (Figure 3.2). However, O_2^{hypo} showed a conspicuous increase with the lowest nitrogen and DOC

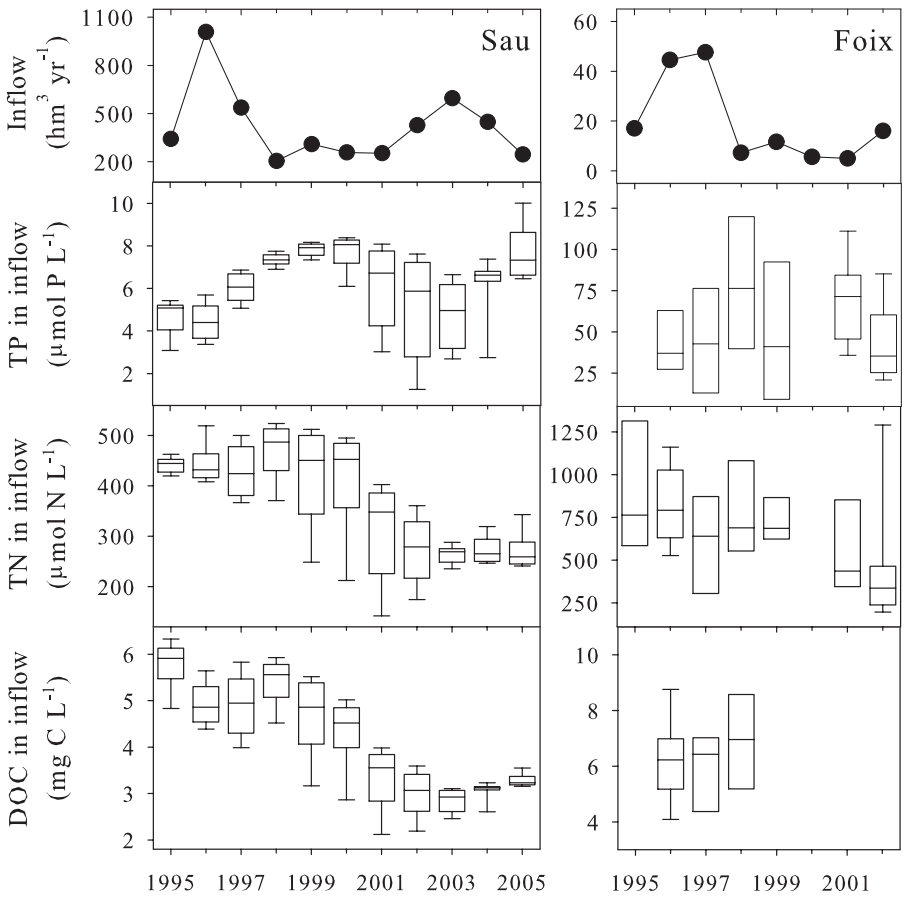

Figure 3.2 – Annual flow and box-whisker plots for measured TP, TN, and DOC concentration in the Ter River (Sau Reservoir tributary, *left*), and in the Foix River (Foix Reservoir tributary, *right*).

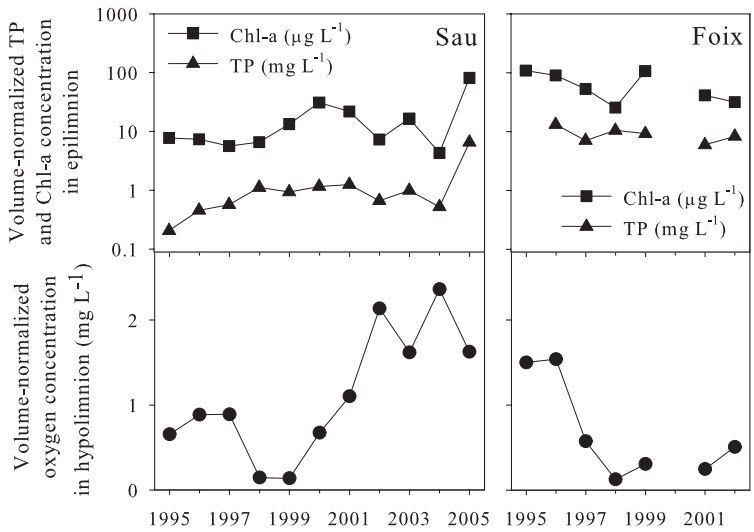

Figure 3.3 – Time trace of epilimnetic TP and *Chl-a* concentrations (*top*), and hypolimnetic oxygen content (*bottom*) in Sau Reservoir (*left*), and Foix Reservoir (*right*). Concentrations are volume-normalized.

inflow, suggesting that river TN and river DOC concentrations could play a role on the hypolimnetic oxygen content. In the case of Foix Reservoir, the evolution of the oxygen content in the hypolimnion did not follow the temporal trend of TP or TN concentration in the river inflow. In any case, although the proxies of the epilimnetic algal biomass showed huge variability in both reservoirs, epilimnetic biomass did not seem to play a principal role shaping the hypolimnetic oxygen content in these reservoirs.

The above interpretation was clearly supported by the results of the empirical regression analysis (Table 3.2). Any variable measured in the epilimnion during summer or spring gave significant results when tested against the oxygen content of the hypolimnion. By contrast, only variables measured in the river inflow were significantly correlated with O_2^{hypo}. Remarkably, in both reservoirs DOC_{inflow} and Cl^-_{inflow} where strongly correlated with O_2^{hypo}, suggesting that human derived organic matter could play a principal role controlling O_2^{hypo}. However, only three data for DOC_{inflow} were available for Foix Reservoir, and interpretations should be cautious in this case. In Sau Reservoir O_2^{hypo} also correlated with TN_{inflow}, but whether this correlation reflects a causal relationship or it was due to the temporal coincidence between DOC and TN river concentration (Figure 3.2 *left panel*, and Table 3.3) could not be inferred from data. The significant relationships in Table 3.2 could not be forced by the influence of hydrology. The summer inflow was not significantly correlated with O_2^{hypo}, and the variables involved in significant correlations did not show significant relationships with summer inflow (Table 3.3), except DOC_{inflow} in Foix Reservoir, that has only three data pairs available.

The control of O_2^{hypo} by external DOC outlined in the preceding analysis was confirmed by the close relationship found between the river DOC load and the oxygen consumption in the hypolimnion. The required assumption of deep intrusion of the river during summer held in both reservoirs (Figure 3.4), with river inflow directly plunging into the hypolimnion or at the metalimnetic level as an interflow in most situations. The relationship between river DOC load and oxygen consumption in Sau hypolimnion (Figure 3.5) was well established in the 1:1 line (slope $= 0.92 \pm 0.09$, n=28, p-value $<$

Table 3.2 – Spearman's τ correlation of volume-normalized mean summer oxygen concentration in the hypolimnion of Sau and Foix reservoirs against selected independent variables (see text for details). *P Value'* stands for the Bonferroni corrected *P Value*. Significance levels below 0.05 are highlighted for clarity.

	Sau Reservoir				**Foix Reservoir**			
	n	Spearman's τ	*P* Value	*P* Value'	*n*	Spearman's τ	*P* Value	*P* Value'
Summer inflow	11	-0.082	0.811		7	0.714	0.071	
TP_{epi}	11	-0.291	0.385		6	0.200	0.704	
SRP_{epi}	11	-0.354	0.285		7	0.500	0.253	
TN_{epi}	11	-0.227	0.501		7	0.714	0.071	
DOC_{epi}	10	-0.139	0.701		3	-0.500	0.667	
Chl-a_{epi}	11	-0.545	0.083		7	0.643	0.120	
Cl^-_{epi}	11	-0.509	0.110		7	-0.143	0.760	
Spring TP_{epi}	11	0.482	0.133		7	0.200	0.667	
Spring SRP_{epi}	11	0.300	0.370		7	0.418	0.350	
Spring TN_{epi}	11	0.009	0.979		7	0.636	0.124	
Spring DOC_{epi}	10	0.164	0.651		5	-0.316	0.604	
Spring Chl-a_{epi}	11	0.354	0.285		7	-0.127	0.786	
Spring Cl^-_{epi}	11	-0.309	0.355		7	0.273	0.554	
TP_{inflow}	11	-0.354	0.285		6	0.257	0.623	
SRP_{inflow}	11	-0.309	0.355		7	-0.286	0.534	
TN_{inflow}	11	-0.891	**<0.001**	**0.004**	7	0.393	0.383	
DOC_{inflow}	11	-0.809	**0.003**	**0.047**	3	-1.000	**0.000**	**0.000**
Cl^-_{inflow}	11	-0.873	**<0.001**	**0.009**	7	-1.000	**0.000**	**0.000**

0.0001, r^2=0.81), strongly supporting that oxidation of riverine *DOC* controls the oxygen content in the hypolimnion. We only had three data pairs in Foix Reservoir, therefore results are not conclusive in this case. But outcomes from this reservoir were not contradictory with results from Sau, with a positive and highly significant relationship between river *DOC* load and oxygen consumption in the hypolimnion (slope = 0.63 ± 0.007, n=3, p-value = 0.007, r^2=0.99). In this case, the slope significantly departed from one, suggesting the presence of important metabolic pathways other than oxygen respiration in this reservoir. However, the extent of the database did not allow to accurately test this supposition.

3.3.2 AF modeling

The results from the different regression equations to predict AF in the four reservoirs consid-

Table 3.3 – Spearman's τ correlation between independent variables involved in significant correlations in Table 3.2, and the summer inflow. The upper side of both correlation matrices contains the sample size in brackets.

	Summer inflow	TN_{inflow}	DOC_{inflow}	Cl^-_{inflow}
Sau				
Summer inflow	-	(11)	(11)	(11)
TN_{inflow}	0.245 ^{ns}	-	(11)	(11)
DOC_{inflow}	0.373 ^{ns}	0.936 ***	-	(11)
Cl^-_{inflow}	-0.245 ^{ns}	0.736 **	0.645 *	-
Foix				
Summer inflow	-	-	(3)	(7)
TN_{inflow}	-	-	-	-
DOC_{inflow}	-1.000 ***	-	-	(3)
Cl^-_{inflow}	-0.714 ^{ns}	-	1.000 ***	-

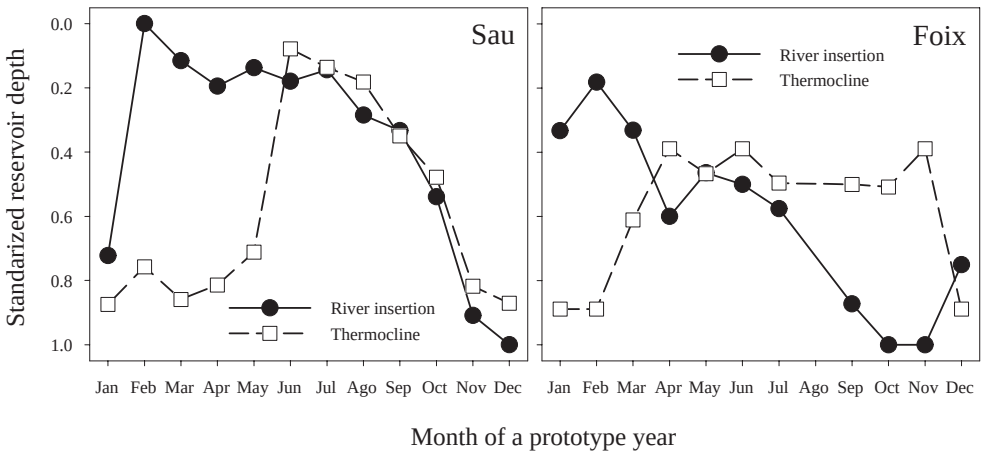

Figure 3.4 – Thermocline and river insertion depth for an average year in Sau Reservoir (*left*) and Foix Reservoir (*right*).

ered are compiled in Table 3.4. Remarkably, where data was available to calculate regressions including variables measured in the epilimnion (i.e., Sau and Foix), we did not find statistical justifications to include these variables in the prediction of AF (*see* Equations 4 to 7, and 10 to 13 in Table 3.4). By contrast, in these reservoirs DOC_{inflow} and Cl^{-}_{inflow} were significant variables explaining the year-to-year variability of AF. In Sau Reservoir the combination of both DOC_{inflow} and Cl^{-}_{inflow} with the summer inflow was statistically supported (Equations 8 and 9), since the partial effects of the independent variables were significant. In Foix Reservoir the combined effect of summer inflow and DOC_{inflow} could not be tested due to the small sample size. But regressions including the summer inflow (Equations 15 and 16) did not support the inclusion of this variable as a significant explaining factor. By contrast, DOC_{inflow} and Cl^{-}_{inflow} explained an outstanding amount of AF variability (i.e., $r^2 > 0.90$, Equations 17 and 18), although in the first case the significance level was badly affected by the small sample size.

In Brownlee Reservoir the dependence of AF on the combination of Cl^{-}_{inflow} and the summer inflow were not supported by available data (Equation 19 in Table 3.4), because these variables were cor-

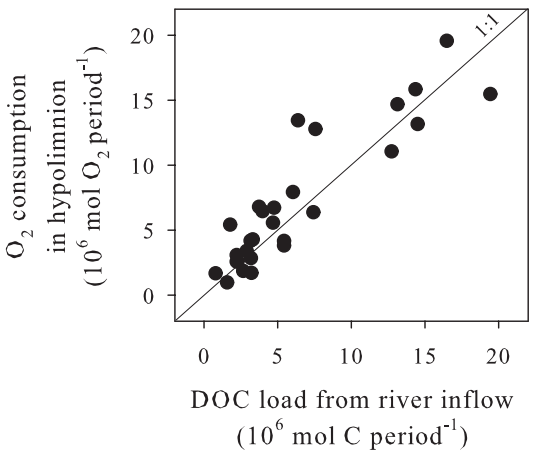

Figure 3.5 – *DOC* load from the Ter River against estimated oxygen consumption in Sau Reservoir hypolimnion in monthly or bimonthly periods.

Table 3.4 – AF modeling results for the four reservoirs considered. All significance levels in this table were calculated with permutation test. Significance levels below 0.05 are highlighted for clarity. Equation 14 was included to avoid confusions.

Equation index	Regression	Whole regression			First independent variable			Second independent variable		
		n	R^2 or r^2	P Value	F-Ratio	P Value	Partial r^2	F-Ratio	P Value	Partial r^2
Sau										
4	AF = 100.15 – 48.93 Inflow + 5.12 TP_{epi}	11	0.40	0.128	4.98	0.070	0.38	1.10	0.360	0.12
5	AF = 98.37 – 40.72 Inflow + 0.11 Chl-a_{epi}	11	0.34	0.175	3.45	0.109	0.30	0.27	0.674	0.03
6	AF = 97.33 – 33.45 Inflow – 0.97 Spring TP_{epi}	11	0.32	0.216	3.65	0.093	0.31	0.01	0.894	0.00
7	AF = 118.60 – 34.80 Inflow – 2.05 Spring Chl-a_{epi}	11	0.50	0.059	5.37	0.061	0.40	2.85	0.126	0.26
8	AF = 52.22 – 57.37 Inflow + 0.18 DOC_{inflow}	11	0.85	**0.002**	37.48	**0.001**	0.82	28.03	**0.002**	0.78
9	AF = 32.33 – 26.11 Inflow + 0.61 Cl^-_{inflow}	11	0.82	**0.002**	8.15	**0.032**	0.50	22.11	**0.003**	0.73
Foix										
10	AF = 79.59 – 64.34 Inflow – 0.67 TP_{epi}	5	0.50	0.497	1.02	0.374	0.34	0.08	0.813	0.04
11	AF = 74.18 – 10.37 Inflow – 0.13 Chl-a_{epi}	6	0.41	0.272	0.22	0.128	0.11	0.36	0.291	0.07
12	AF = 64.08 – 21.84 Inflow + 0.35 Spring TP_{epi}	6	0.35	0.546	1.53	0.280	0.33	0.07	0.800	0.02
13	AF = 63.77 – 20.33 Inflow + 0.06 Spring Chl-a_{epi}	6	0.39	0.540	1.73	0.292	0.37	0.23	0.822	0.07
14	AF =105.74 – 176.49Inflow – 2.79 DOC_{inflow}	3	-	-	-	-	-	-	-	-
15	AF = 32.97 – 0.77 Inflow + 0.11 Cl^-_{inflow}	6	0.91	**0.021**	0.01	0.922	0.00	18.82	**0.025**	0.86
16	AF = 67.75 – 19.81 Inflow	6	0.34	0.175	-	-	-	-	-	-
17	AF = -21.36 + 11.41 DOC_{inflow}	3	0.98	0.177	-	-	-	-	-	-
18	AF = 32.34 + 0.12 Cl^-_{inflow}	6	0.91	**0.011**	-	-	-	-	-	-
Brownlee										
19	AF = 47.52 – 0.0006 Inflow + 2.23 Cl^-_{inflow}	7	0.80	**0.049**	0.26	0.654	0.06	2.82	0.150	0.41
20	AF = 121.34 – 0.0020 Inflow	7	0.65	**0.031**	-	-	-	-	-	-
21	AF = 26.34 + 2.81 Cl^-_{inflow}	7	0.78	**0.010**	-	-	-	-	-	-
Pueblo										
22	AF = 54.38 – 0.001 Inflow + 12.9 DOC_{inflow}	5	0.77	0.147	6.56	0.061	0.77	0.21	0.739	0.09
23	AF = 25.18 – 0.011 Inflow + 1.37 Cl^-_{inflow}	11	0.80	**0.001**	12.97	**0.008**	0.62	0.32	0.587	0.04
24	AF = 33.40 – 0.012 Inflow	20	0.74	**0.001**	-	-	-	-	-	-
25	AF = 53.11 – 11.820 DOC_{inflow}	6	0.23	0.360	-	-	-	-	-	-
26	AF = -19.59 + 7.590 Cl^-_{inflow}	11	0.48	**0.024**	-	-	-	-	-	-

related (Spearman's $\tau = -0.86$, p-value $= 0.014$, $n = 7$). This makes difficult the precise separation of the partial effects of these variables on AF prediction. However, partial r^2 values for Equation 19, and results from Equations 20 and 21 suggest that Cl^-_{inflow} has an important role on AF variability. By contrast, in Pueblo Reservoir the summer water inflow was the only significant variable (Equations 23 and 24, partial significance for this variable in Equation 22 seems to be badly influenced by the sample size). DOC_{inflow} (Equation 25) and Cl^-_{inflow} were not considered relevant, despite the significant correlation between Cl^-_{inflow} and AF (Equation 26). Considering partial r^2 values in Equation 23, and the correlation between summer inflow and Cl^-_{inflow} (Spearman's $\tau = -0.81$, p-value $= 0.003$, $n = 11$), results in Equation 26 are mostly attributed to the effect of summer inflow on Cl^-_{inflow} values.

3.4 Discussion

The results from Sau and Foix reservoirs clearly shows that the summer hypolimnetic oxygen content in these water bodies are largely controlled by external *DOC* inputs. The significant correlations between oxygen content and Cl^- (Table 3.2) supports the conclusion that *DOC* carried by the river inflows is mainly from human origin. Thus, human derived spills directly controls the hypolimnetic oxygen content in these reservoirs, and organic matter produced in the epilimnion did not appear to be a key factor. From a theoretical point of view this has remarkable implications, because despite the fact that the effect of external *DOC* inputs on hypolimnetic oxygen have been considered in some classical studies (Hutchinson 1957; Nürnberg 1995), virtually all the empirical models considering processes in the hypolimnion are based on the assumption that the key driving process is the decay of organic matter sinking from the epilimnion. A general advice coming from our results is that assumptions of classical models concerning the oxygen content in the hypolimnion do not necessarily hold in reservoirs under strong human impact.

The above conclusion also reaches other hypolimnetic processes that are essentially dependent on the hypolimnetic oxygen concentration. The internal load of phosphorus is a good example, since it is usually modeled as a function of some measure of lake productivity or of the anoxia extent (Carpenter et al. 1999; Nürnberg and LaZerte 2004). Obviously, if the oxygen concentration is dependent on the external *DOC* input, internal load of phosphorus will also be dependent on it to some extent. This is very interesting from a management point of view, because it means that in some circumstances one of the key processes governing water quality resilience of temperate water bodies (Folke et al. 2004) are linked to a process that could be directly controlled by human intervention in the watershed (i.e. reducing *DOC* load from human related spills). That is, we can reduce oxygen consumption considering a first order process related to *DOC* input, without the need to deal with the frequently non-linear, complex relationship between nutrient load reduction, algal biomass response, and concomitant reduction in oxygen consumption. Also, the hypolimnetic oxygen control by external *DOC* inputs are a possible explanation of some disappointments of lake recovering programs based on nutrient load reduction (*see* Cooke et al. 1993).

Results from the AF modeling analysis suggest that at least in reservoirs the effect of allochthonous *DOC* input on the hypolimnetic oxygen content depends on the lability of *DOC* entering the waterbody, which is not at odds with the current observation that bacterial metabolism are not well correlated with bulk dissolved organic matter (Findlay 2003). This view was supported by the relative importance of hydrology and Cl^-_{inflow} on AF prediction (Figure 3.6). While in the most impaired reservoir (Foix Reservoir, Figure 3.6A and B) AF variability could exclusively be explained by the proxy of organic matter lability (i.e. Cl^-_{inflow}, *see* Figure 3.1), as we move to reservoirs less influenced by human related spills the importance of allochthonous materials on AF decreases, and the relevance of hydrology increases (Figure 3.6 and Table 3.4). That is, as the $C : N$ ratio of the organic matter entering the reservoir decreases, the relevance of the oxidation of these materials on the hypolimnetic oxygen

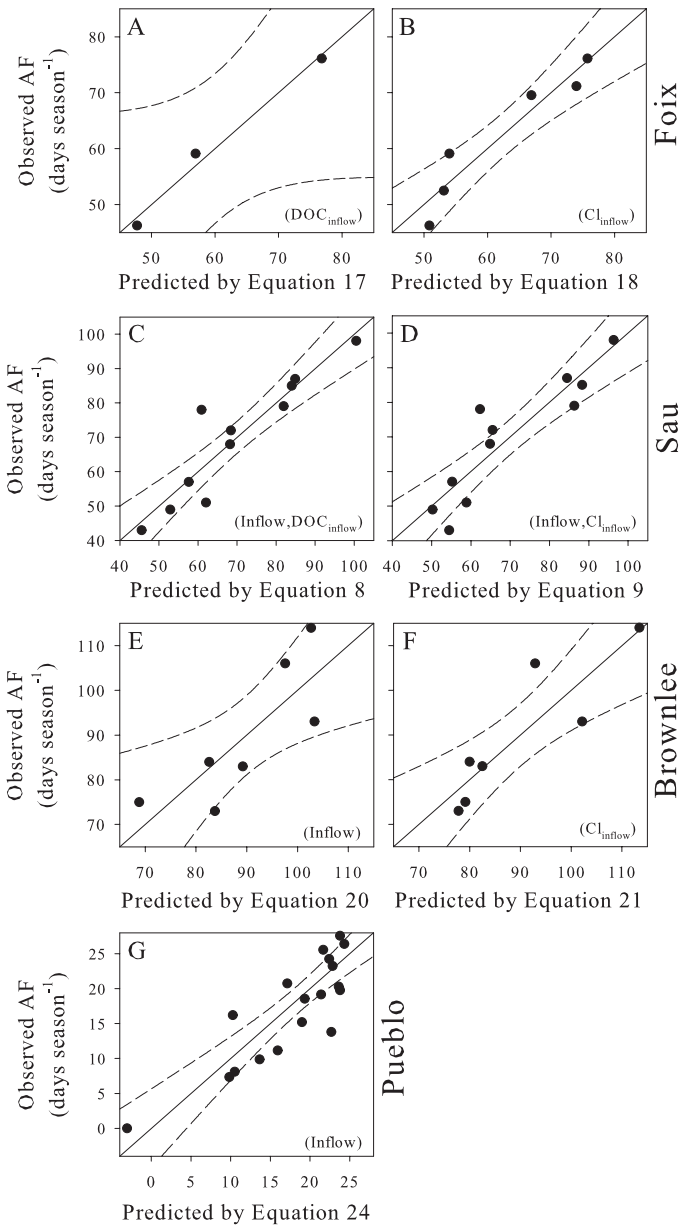

Figure 3.6 – AF predictions (regression line and 95% confidence intervals) in (A, B) Foix Reservoir, (C, D) Sau Reservoir, (E, F) Brownlee Reservoir, and (G) Pueblo Reservoir. Equation numbers refer to equations in Table 3.4. Independent variables included in the equation are given in brackets at the bottom of each panel. Panels were arranged to place reservoirs in a gradient of relative human impact (Foix Reservoir at the top, Pueblo Reservoir at the bottom).

content increases. This is coherent in reservoirs, because these systems have short water residence times (Table 3.1), and only materials that decay in a time scale equal or shorter than that of the water retention time will be relevant for carbon and oxygen cycling. Water retention time in reservoirs is typically below one year, and values less than 100 *days* are frequently recorded (Table 3.1). Considering that only the most labile *DOC* fractions are consumed in these time scales (del Giorgio and Davis 2003), it is reasonable to predict that in these rapidly flushed systems only the labile *DOC* fractions will be relevant for carbon and oxygen dynamics. Although our database did not allow to fully demonstrate this hypothesis, results from the AF modeling seem to point in this direction. Reservoirs receiving organic matter with low $C:N$ ratios (i.e. Sau and Foix reservoirs, Figure 3.1) showed significant DOC_{inflow} effects (Equations 8 and 17), while in the reservoir showing the highest $C:N$ ratio in inflowing organic matter (Pueblo Reservoir, Figure 3.1) DOC_{inflow} was a non significant factor (Equations 22 and 25).

Conclusions outlined above make an extensive study of the allochthonous *DOC* effect on hypolimnetic oxygen in reservoirs desirable. In principle, the effect of external *DOC* inputs on the hypolimnetic oxygen content of lakes has been already tested by Nürnberg (1995). She concluded that although the external *DOC* load largely explained the year-to-year variability of AF in single lakes, this variable did not have any significant effect on between lakes AF prediction. However, the last statement was supported by the lack of relationship between *DOC* load and AF including only a small subset of lakes (p-value < 0.32, $n = 8$). Interestingly, if we reevaluate the relationship from which one of the most influential conclusions in Nürnberg's paper were draw (TP loading against lake AF, $r^2 = 0.76$, p-value < 0.0001, $n = 17$), but considering only this subset of lakes, the effect of TP loading vanishes ($r^2 = 0.005$, p-value $= 0.873$, $n = 8$). Our intention is not to diminish the value of Nürnberg's (1995) study, because several analyses in this paper confirmed the importance of TP on AF prediction, and she already noticed the possible effect of *DOC* load if more samples were available. But in our opinion we still lack a conclusive cross-sectional study on the effect of allochthonous *DOC* on the oxygen content of lakes and reservoirs.

To conclude, results from this work emphasizes that the role of allochthonous inputs in determining hypolimnetic dissolved oxygen concentrations has not received nearly the attention that epilimnetic primary production and TP have received. However, allochthonous *DOC* can be a very important driver in reservoirs under strong human impact. This should prompt practitioners to test the possible effect of organic matter entering the system when dealing with impaired waters. Also, the hypolimnion layer of reservoirs should be regarded as a system potentially opened to their watershed. This should always be considered when formulating empirical models for these systems.